THESIS

REACTOR DESIGN FOR ELECTROCHEMICAL OXIDATION OF THE PERSISTENT ORGANIC POLLUTANT 1,4-DIOXANE IN GROUNDWATER

Submitted by

P. Maxine Cottrell

Department of Civil and Environmental Engineering

In partial fulfillment of the requirements

For the Degree of Master of Science

Colorado State University

Fort Collins, Colorado

Spring 2018

Master's Committee:

Advisor: Jens Blotevogel
Co-Advisor: Tom C. Sale

David Dandy

ABSTRACT

REACTOR DESIGN FOR ELECTROCHEMICAL OXIDATION OF THE PERSISTENT ORGANIC POLLUTANT 1,4-DIOXANE IN GROUNDWATER

The common industrial solvent stabilizer and wetting agent 1,4-dioxane (DX) is one of the most widely occurring organic groundwater contaminants in the United States today. It is a probable human carcinogen, highly mobile in groundwater, and resistant to anaerobic biodegradation. The ineffectiveness of conventional treatment approaches such as stripping and sorption to activated carbon results in a critical need of advanced technologies for the treatment of DX in groundwater. Previous studies have shown that electrochemical oxidation is able to fully mineralize 1,4-dioxane, but testing has thus far been limited to proof-of-principle bench-scale experiments. Consequently, this study addresses the design of a configurable mobile pilot-scale reactor that can be used to test electrochemical degradation performance under site-specific conditions and with different dimensionally stable electrode materials. The goal of this reactor design is to accommodate straightforward scale-up for field applications, and low cost of production so that ultimately multiple modular units can be deployed to operate in series or in parallel.

Assessment of critical design parameters in a bench-scale reactor showed that DX degradation rates almost doubled when no inter-electrode solid media were used. No significant differences were observed between operating the reactor in continuous versus batch mode. An additional 57% degradation rate improvement was achieved when the batch reactor was operated with 30-minute polarity reversals as compared with constant polarity.

Bench-scale reactor and initial pilot reactor tests with Ti/IrO_2-Ta_2O_5 electrodes were run using a synthetic groundwater solution containing DX in NaCl electrolyte, revealing substantial effects of scale, while DX degradation kinetics were similar. Groundwater from a contaminated industrial site was then treated in the pilot reactor with an apparent anode surface area per order of magnitude DX removal (ASA_{AO}) of 305 $h*m^2/m^3$ at an electric energy consumption per order of magnitude DX removal (E_{EO}) of 152 kWh/m^3, with relatively minor production of undesirable by-products.

The contaminated site groundwater was also treated in a commercial bench-scale reactor with a Magnéli-phase titanium oxide anode, resulting in an ASA_{AO} of 28 $h*m^2/m^3$ at an E_{EO} of 176 kWh/m^3, but with a high yield of carbon tetrachloride (CCl_4) and chlorate (ClO_3^-), and minor formation of perchlorate (ClO_4^-). In comparison of the surface-area normalized rates of removal, the commercial reactor was faster than the pilot reactor, but it consumed more energy per order reduction and generated more undesirable reaction by-products, commonly referred to as disinfection by-products (DBPs).

Future testing at contaminated field sites will reveal the efficacy of this newly designed reactor, and thus electrochemical treatment, for the remediation of groundwater contaminated with DX and other persistent organic pollutants.

TABLE OF CONTENTS

LIST OF TABLES

LIST OF FIGURES

1. INTRODUCTION

1.1. Background

Past industrial practices and manufacturing process upsets have led to the release of toxic compounds into the environment. Many of these chemicals are water-soluble organics that are relatively stable in the subsurface environment. These compounds include pesticides, dye stuffs, solvents, and industrial chemistry by-products of various elemental composition, for example polycyclic aromatic hydrocarbons, perfluorinated compounds, dioxins, dioxane, and others. When these toxic pollutants spread with natural groundwater flow, they may pose serious environmental and human health risks, thus, active remedies are sometimes needed to eliminate the pollutants, especially for compounds which do not readily degrade to non-toxic products.

Extensive work has been done over the past few decades to develop processes that will break down and mineralize persistent organic compounds, thus removing the hazard they present in groundwater. Common traditional groundwater treatment methods studied or implemented for organic contaminants have been excavation and incineration, *in situ* thermal treatment, soil vapor extraction (SVE), and biological treatment (Brusseau, Carroll, et al., 2013; Gomes, Dias-Ferreira, et al., 2013; Heron, Parker, et al., 2015; Kang, 2014; Laine & Cheng, 2007; Weber, Watson, et al., 2011; Wenzel, 2009). Advanced oxidation processes (AOPs) are a family of treatments which introduce strong oxidizing agents to the contaminants, typically through UV irradiation, ozonation, or chemical addition to promote reactions that lead to mineralization of the contaminant (Rajeshwar, Ibanez, et al., 1994). Electrochemical oxidation is an AOP where electron transfer occurs through generation of reactive oxygen species or directly at the surface of the anode. This technology is capable of degrading a wide range of organic contaminants, requires no auxiliary

chemicals, does not produce waste, and is more easily adjusted to variations in influent composition than other AOPs (Radjenovic & Sedlak, 2015). However, most studies on electrochemical treatment have thus far been conducted at a bench scale, and insights on technology scale up are critically lacking. Thus, the design and testing of a pilot-scale electrochemical reactor was the primary objective of this research.

The model compound for this research was the organic solvent 1,4-dioxane (Figure 1), often simply referred to as dioxane (DX). Dioxane has been widely used in industry for most of the second half of the 20th century as a stabilizing agent for chlorinated solvents (Anderson, Anderson, et al., 2012; Mohr, Stickney, et al., 2010). As described in several patents, DX's role in its chlorinated co-solvents was to temper their instability in the presence of metals, thereby reducing corrosion (Bachtel, 1957; Petering & Aitchison, 1945; Rapp, 1960). As a manufacturing by-product, 1,4-dioxane is also present in some industrial waste streams and as an impurity in some household products (DiGuiseppi, Walecka-Hutchison, et al., 2016; Mohr et al., 2010; NHDES, 2011; Teaf & Garber, 2015; USEPA, 2017a). Because of its extensive use prior to the enactment of laws limiting the handling and disposal of hazardous chemicals, DX along with its co-solvents has made its way into groundwater at many current and former industrial sites and military installations in the USA. Once DX gets into the groundwater, it largely stays dissolved and is very difficult to remove. Dioxane was not understood to be a threat to human health until fairly recently when it was classified as probable human carcinogen by the World Health Organization (WHO) and by the U.S. Environmental Protection Agency (EPA) after confirming its carcinogenicity in animal studies (ACGIH, 2015; GAMAP, 2009; Mohr et al., 2010; NHDES, 2011; Teaf & Garber, 2015; USEPA, 2014). In 2011, the WHO set a DX limit of 50 micrograms per liter (μg/L) in drinking water (Villanueva, Kogevinas, et al., 2014). The EPA has not yet established an

enforceable maximum contaminant level (MCL) on this compound but has set a health advisory level of 35 parts per billion (35 µg/L) dioxane in groundwater. As of 2015 several U.S. states have set regulatory guidelines for dioxane levels from 0.25 to 200 µg/L in groundwater or drinking water (CWQCC, 2016; Lewis, 2014; Suthersan, Quinnan, et al., 2016; USEPA, 2014, 2017b).

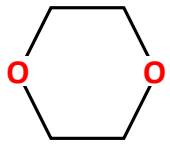

Figure 1 Molecular structure of 1,4-dioxane.

Sampling results reported in the EPA's third Unregulated Contaminant Monitoring Rule (UCMR 3) show that DX has been identified at concentrations higher than a 0.35 µg/L reference standard in about 7% of the public water supplies (PWS) tested, and at levels greater than the minimum reporting limit of 0.07 µg/L in more than 20% of the PWS tested (Adamson, Piña, et al., 2017; DiGuiseppi et al., 2016; Suthersan et al., 2016; USEPA, 2017d). Observations at a number of contaminated sites indicate that DX is likely to be present at elevated concentrations, but at many of these sites testing was not done for DX, so its presence has not yet been reported (Adamson, Mahendra, et al., 2014).

Biodegradation of 1,4-dioxane under anoxic conditions has not yet been observed, and typical SVE approaches that might be effective for volatile organics removal are not effective for DX removal. Other traditional treatments such as sorption to activated carbon have likewise proven ineffective at cost-effectively reaching the low target concentration limits dictated by public health regulations for this challenging contaminant. Given the nature of dioxane, treatment with electrochemical AOP may be a cost-effective environmentally benign approach to addressing the threat DX poses to our health via our groundwater.

1.2. Objectives

The principle objective of this work was to design and evaluate a configurable pilot-scale electrochemical reactor with respect to treatment of groundwater from a 1,4-dioxane-contaminated site. Specific objectives were to:

- design and test different configurations in a bench-scale electrochemical reactor,
- test a scaled-up version of the configurable electrochemical reactor using both synthetic groundwater and genuine contaminated groundwater through analysis of reaction kinetics,
- compare the scaled-up version of the designed electrochemical reactor with a commercial electrochemical reactor, and
- quantify the formation of undesirable reaction by-products.

1.3. Organization of this document

This document is divided into six chapters:

Chapter 2: Literature review – The review presents the current state of knowledge regarding electrochemical treatment and identifies knowledge gaps.

Chapter 3: Bench-scale reactor – The third chapter contains a detailed description of the bench-scale reactor design, experimental methods and results, and a discussion of important findings.

Chapter 4: Pilot-scale reactor design and performance – The fourth chapter describes the pilot-scale reactor design, experimental methods and results, and a discussion of the findings.

Chapter 5: Performance comparison with commercial test reactor – The fifth chapter presents experimental methods and results with a commercial bench-scale reactor using a different type of electrode. Results from the two reactor results are compared and discussed.

Chapter 6: Conclusions – Important conclusions from the laboratory studies are discussed in this chapter.

Chapter 7: Future Work – Suggestions for future studies are outlined in this chapter.

Chapter 8: *References*

Appendix – The appendix includes raw data and calibration information.

2. LITERATURE REVIEW

2.1. Treatments for 1,4-dioxane in contaminated groundwater today

As awareness of the risks associated with DX in groundwater has grown, various methods and technologies have been implemented in attempts to remove or degrade this compound. Some U.S. states have recognized DX as a contamination issue for ten years or more, but only in the past couple of years has it been more widely understood by private and public sector parties to be a public health threat that needs to be addressed (Suthersan et al., 2016). The dioxane molecule has a pair of ethers linked symmetrically in a ring form, allowing the molecule to have a high degree of stability and making it more resistant to reaction with acids and oxidizing agents than other $C_4H_8O_2$ isomers (Mohr et al., 2010). The goal for treating many contaminants in groundwater, including DX, is to achieve full mineralization of the compound. In the process of the transformation from dioxane to carbon dioxide the cyclic ether is initially broken open, making it more amenable to subsequent oxidation.

Soil vapor extraction (SVE) is a common physical treatment for some vadose zone organic pollutants, but is ineffective on compounds like DX with a Henry's law constant (K_H) less than 1 L*atm/mol at ambient temperatures and pressures (DiGuiseppi et al., 2016; Mohr et al., 2010). The affinity for water over air represented by a low K_H means DX will tend to travel with water out of the vadose zone and into the saturated zone, where SVE is not effective. To present a broad picture of the various treatment methodologies currently in use or being investigated for treatment of DX in groundwater at source zones and in plumes, Table 1 lists some of the main treatments that have been deployed or are still in development (Suthersan et al., 2016). Treatments listed may have been studied or implemented in combination with each other.

Table 1 A non-exhaustive sampling of treatment methods and selected references for the removal of 1,4-dioxane from groundwater. Table adapted from "Making Strides in the Management of "Emerging Contaminants" by Suthersan et al. (2016). Technology development levels are categorized as follows: implemented: several examples of field-scale or commercial application are available; in development: literature addresses lab or pilot-scale reports without documented commercial application; insufficient data: data too limited to document the treatment mode.

Treatment mode	Additional information and references	Level of technology
Ultrafiltration	not used due to cost and non-destructive nature of treatment	insufficient data
Thermal	presumed not to be used to target DX due to cost and broad reach of DX-contaminated plumes (Davis, 1997; Heron et al., 2015; Oberle et al., 2015)	in development
Sorption onto media	presumed not commonly used due to its non-destructive nature (B. DiGuiseppi et al., 2017; W. DiGuiseppi et al., 2016; Favara et al., 2016; Woodard et al., 2014)	in development
Sono-chemical	ultrasonic waves promote formation of radical species (Beckett et al., 2001; Chitra et al., 2012; B. Li et al., 2016; Nakajima et al., 2004; Sathishkumar et al., 2016)	in development
Biological	microbial treatments (Lippincott et al. 2015, Mahendra and Alvarez-Cohen 2006, Mora & Chiang, 2014)[1], (Chiang et al., 2012; Sekar et al., 2014; USEPA, 2014) photosynthesizing plants (Aitchison et al., 2000; Ferro et al., 2013)	implemented and in development
Advanced oxidation processes		
Chemical oxidation	activated persulfate, (B. Li et al., 2016; Yan et al., 2016) peroxone (hydrogen peroxide (H_2O_2) and ozone (O_3)) (Eberle et al., 2016; Ghatak, 2014)	implemented and in development
Electro-chemical	Electrochemical generation of hydroxyl radicals, done alone or in combination with added oxidizing agents (e.g. H_2O_2 and/or O_3) or catalysts (e.g. titanium dioxide, TiO_2) (Anglada et al., 2009; Brillas et al., 2003; Jasmann et al., 2016a; Kishimoto et al., 2008; Sirés et al., 2014; Wang, 2017; W. Wu et al., 2014)	in development
Photolytic	UV alone and in combination with O_3 and/or H_2O_2, UV activation of photocatalysts (e.g. TiO_2) (Chitra et al., 2012; Ghatak, 2014; Hill et al., 1997; Kwon et al., 2012; Legrini et al., 1993)	implemented and in development

Ultrafiltration (UF):

UF application may be useful for removing some contaminants, e.g. perfluorinated compounds, from treated drinking water, but because UF membrane pores are so small, for raw groundwater

treatment the level of filtration required to remove solids upstream of the UF membranes is not insignificant. The upstream removal step is required to avoid blinding or plugging of the UF membranes. Given that DX is a relatively small molecule, the pre-filtration steps alone required for ultrafiltration treatment make it an unreasonable option.

Thermal treatment:

Thermal treatment, also called thermal desorption and degradation, has historically been applied to excavated soils. The incineration of excavated soils may effectively combust sorbed contaminants, but is not effective in treating the groundwater, and presents additional routes of contaminant exposure as well as drastically impacting the soil surface. Updated *in-situ* thermal treatment techniques involve heating the subsurface by insertion of a series of conductive elements, or by injection of steam or hot water, and can be used under and around structures (Davis, 1997; Heron et al., 2015). Davis cites reports by Fulton et al. (1991), Davis and Lien (1993), US EPA (1995), and Newmark and Aines (1995) that when these thermal treatment techniques are applied appropriately they can be effective to remediate organic contaminants. Work done by Oberle and team at lab scale and at a field site indicate some success with electrical resistance heating at reducing subsurface concentrations of DX during site treatment for chlorinated organics contamination, but the researchers acknowledge that there is not complete evidence that DX was mineralized (Oberle, Crownover, et al., 2015). The inference is made that DX was steam stripped from the contaminated groundwater as a result of the applied heat. A benefit of *in situ* thermal treatment is that no chemicals need to be added to the subsurface. Drawbacks however include availability of the heating medium (power, steam, hot water), and the capital and operational expense of infrastructure required to deliver the heat to specific contamination concentrations in the subsurface and to collect produced volatile organic compounds. According to Stewart and

Udell (1988) as reported by Davis, another problem with thermal treatment using hot water is the risk of increased residual water saturation which may allow highly soluble contaminants such as 1,4-dioxane to remain in the subsurface soil-water matrix (Davis, 1997).

Sorption:

To allow groundwater contaminants to be removed by sorption to *ex situ* media, groundwater must be pumped to a unit containing the sorbent material, allowed adequate time at appropriate pressure and temperature for the sorption to occur, then the groundwater is presumably pumped back into the subsurface. The sorbent media, once it is loaded with the contaminant, either must be completely incinerated or it may be regenerated by exposing it to elevated temperature via steam, for example. DX tends not to sorb to surfaces, particularly soil surfaces, which is why it is so mobile in groundwater and which is why, aside from a reported application in 2003, GAC is minimally effective as a sorbent for groundwater dioxane (DiGuiseppi, Hatton, et al., 2017; DiGuiseppi et al., 2016; Mohr et al., 2010; USEPA, 2006; Zenker, Borden, et al., 2003). DiGuiseppi and co-authors (2017) report that after testing several synthetic carbonaceous resins unsuccessfully, they found a proprietary divinylbenzene-based product made by Dow Chemical, AMBERSORB™, which has been demonstrated at multiple sites with >99% removal rates for high starting concentrations of DX ($\leq$ 40 mg/L). Woodard's work supports this finding with three successful case studies (Woodard, Mohr, et al., 2014). This sorbent compound is used as part of a system that requires media regeneration, but reportedly is cost-effective as part of a pump and treat system (Favara, Tunks, et al., 2016). The main drawback to sorption as a treatment method is that it concentrates and transfers the contaminant to a different media, but it does not mineralize it. The other major drawbacks are the capital and operating costs for the multiple unit operations required by the system and its media regeneration needs.

Sonochemical treatment:

Sonochemical treatment is an *ex situ* method that exposes contaminated groundwater to ultrasonic waves. These waves induce acoustic cavitation due to the expansion and compression cycles of the sound waves in water (Beckett & Hua, 2001). This action leads to the generation of very high temperatures and pressures within microbubbles, as well as the generation of free radicals (Beckett & Hua, 2001; Hung & Hoffmann, 1999; Nakajima, Tanaka, et al., 2004; Sathishkumar, Mangalaraja, et al., 2016). The target contaminant in sonochemical treatment may be mineralized directly by $^{\bullet}OH$ oxidation, pyrolytic degradation, or by supercritical water reactions (Hung & Hoffmann, 1999). As with other groundwater treatment methods, sonochemical techniques have been combined in the laboratory with photolysis, catalysts, and reagents (e.g. Fenton's reagent and persulfate) to increase the effectiveness of treatment (Chitra, Paramasivan, et al., 2012; B. Li & Zhu, 2016; Nakajima et al., 2004; Sathishkumar et al., 2016). Though this treatment mode can be very effective at contaminant destruction, its energy requirements are high and may be cost prohibitive, and it is not evident that the specialized equipment it requires has been sized for or tested in field applications at this time.

Biological treatment:

Biological and biochemical treatments employing living organisms ranging from microbes to trees for the degradation and removal of 1,4-dioxane can be either *ex situ* or *in situ* depending on the technology selected and the application environment. Within this family of treatments are bioreactors, co-metabolic biological treatment, microbially-driven Fenton reactions and at a more macro-scale, phytodegradation. Biological degradation, including monitored natural attenuation (MNA), theoretically only requires an active population of microbes that can (co-)metabolize and mineralize the pollutant. DX, however, is known to be "relatively resistant to biodegradation"

(USEPA, 2014) in the anoxic environment of subsurface groundwater, but it is not completely impervious to degradation, particularly in aerobic conditions (Adamson, Newell, et al., 2017; USEPA, 2014; Zhang, Gedalanga, et al., 2017). An environmental remediation contractor, CH2M, has effectively used classic *ex situ* industrial waste water treatment systems to create a treatment bioreactor that promotes aerobic stimulation of dioxane-degrading bacteria. After a series of successful systems tests, the company has gone on to create bioreactors for DX treatment at multiple sites, with at least one full-scale treatment system in continuous operation since 2006 (DiGuiseppi et al., 2016). Some work has been done considering *in situ* biodegradation, showing that there are some bacteria strains which are able to metabolize or co-metabolize DX, but that the effectiveness is limited by the presence of the pervasive co-contaminants TCA and DCE (Adamson, Newell, et al., 2017; Mahendra, Grostern, et al., 2013; Zhang et al., 2017). *In situ* biological treatments involve injection of amendments such as oxygen, microbial cultures, carbon sources for co-metabolic degradation (e.g., propane), and possibly other nutrients to promote specific microbial activity. Enhanced anaerobic bioremediation has been studied by Shen and co-workers who report DX degradation in the presence of wastewater treatment sludge enriched with Fe^{3+} and Fe^{3+}-reducing bacteria (Shen, Chen, et al., 2008).

Research has been done on microbially-driven Fenton reactions, where peroxide formation is a result of microbial respiration and Fe(II) is formed from microbial reduction of Fe(III), allowing the H_2O_2 and Fe^{2+} reaction to generate hydroxyl radicals without the requirement to add these compounds directly (Sekar & DiChristina, 2014; Sekar, Taillefert, et al., 2016). Despite lower degradation rates using this method as compared with adding reagents directly, this microbially-driven approach is promising because the supply, transportation, and storage of chemicals involved in Fenton reactions, particularly H_2O_2, present costs and risks that the microbially-driven process

can avoid. However, the work to date has been done only at lab scale, and has not been field-tested in the presence of natural soils, where the concentrations of iron species are not controlled.

The treatment of contaminants by plants is known as phytodegradation or phytoremediation. In this area Ferro, Aitchison, Chiang and others have shown that poplars and willows can take up DX from groundwater and mineralize it effectively without build-up in the plants' cells (Aitchison, Kelley, et al., 2000; Chiang, Anderson, et al., 2016; Chiang, Mora, et al., 2012; Ferro, Kennedy, et al., 2013). A key limitation of phytoremediation is the treatable concentration: if the dioxane concentration is too high it will damage the plant, sometimes fatally. For this reason phytoremediation may best be considered for plume treatment or as a finishing step for other treatment.

MNA is included here for the sake of thoroughness because although natural attenuation is not an imposed treatment, it is a tool that is being investigated for some DX-contaminated sites as part of a holistic groundwater remediation process (Adamson, Anderson, et al., 2015; Adamson, Newell, et al., 2017; Chiang, Glover, et al., 2008; Mahendra et al., 2013). Aerobic bioremediation by bacteria and by fungi is being studied to better understand and model natural attenuation timelines for DX degradation (Adamson, Newell, et al., 2017; Nakamiya, Hashimoto, et al., 2005; Zhang et al., 2017).

Advanced oxidation processes:

Combustion via high temperature incineration is one of the oldest historical means of disposing of pollutants. Combustion as a general term indicates full mineralization of the compound to its most elementary form, carbon dioxide (CO_2). But combustion via incineration requires fuel along with specialized equipment, typically not mobile, and can result in combustion products or by-products that are sometimes more harmful than the starting pollutant, so though this is still a

treatment or disposal method in some cases, it is not cost effective for extensive groundwater treatment.

Chemical oxidation is another form of combustion. Ambient combustion or conversion of pollutants leads to mineralization through oxidation reactions at ambient temperature and pressure. When the oxidation treatment involves very strongly oxidizing agents, such as ozone (O_3), hydrogen peroxide (H_2O_2), or hydroxyl radical ($^{\bullet}OH$), this is known as an advanced oxidation process, or AOP (Aieta, Reagan, et al., 1988; Fleming, 2000; Ghatak, 2014).

AOPs work by promoting the formation of active oxidants. For example, common AOPs include use of H_2O_2 in combination with ferrous iron (Fe^{2+}) which react to form $^{\bullet}OH$, ozone (O_3) with H_2O_2 subjected to UV light which react to form $^{\bullet}OH$, and/or permanganate as an oxidant, or titanium oxide (TiO_2) as a catalyst.

Photolytic AOP treatments use UV to react with water, liberating reactive $^{\bullet}OH$ which oxidize the target compounds, leading to mineralization. A drawback to photolytic AOP may be limited UV penetration to the entirety of the solution, increasing cost due to equipment design and power requirements for pumping and treatment (Legrini, Oliveros, et al., 1993).

2.2. Electrochemical treatment of contaminated waters

AOPs in general are typically expensive because they require transportation, delivery and safe storage of the reagents as well as personnel to operate and maintain the equipment (Butkovskyi, Jermaisse, et al., 2014; Martínez-Huitle & Ferro, 2006; Martínez-Huitle & Rodrigo, 2015; Panizza & Cerisola, 2009). Electrochemical AOPs (EAOPs), however, use electricity in combination with electrodes as the electron source to oxidize water at the anode, freeing up $^{\bullet}OH$ to react with contaminant species. Electrochemical treatment techniques are able to introduce the electron

cleanly and safely, without chemical transport and storage issues, and without introducing additional inherent toxicity into the environment (Brillas, Cabot, et al., 2003).

EAOPs have been widely studied for treatment of landfill leachate and industrial waste waters, particularly in some food processing and pharmaceutical production applications (Ahsan, Kamaludin, et al., 2014; Anglada, Urtiaga, et al., 2009; Gotsi, Kalogerakis, et al., 2005; Klančar, 2016). In the case of treatment of olive oil mill waste water, it was found that despite good results with destruction of the target contaminants, mainly phenols and tannins, undesirable organo-chlorinated by-product concentrations increased to an unacceptable level (Gotsi et al., 2005). Chopra and co-authors provide an overview of EAOP technology and discuss operating costs, which must not be ignored when evaluating any treatment system (Chopra, Sharma, et al., 2011).

Building on work done for wastewater and landfill leachate treatments using electrochemical oxidation, several researchers have investigated the application of electrochemical oxidation for degradation of a variety of persistent organic contaminants, as reported in a series of thorough review papers (Deng & Englehardt, 2006; Ghatak, 2014; Martínez-Huitle & Ferro, 2006; Martínez-Huitle & Rodrigo, 2015; Moreira, Boaventura, et al., 2017; Rajeshwar et al., 1994). In all of these studies, the anode in an electrolytic cell is used to oxidize the target compound (Butkovskyi et al., 2014; Moreira et al., 2017; Radjenovic & Sedlak, 2015). There are two modes of anodic oxidation: direct and indirect oxidation (Martínez-Huitle & Ferro, 2006; Radjenovic & Sedlak, 2015). In the former, the oxidation reaction occurs directly at the anode surface where the target compound undergoes electron transfer or reacts with surface-associated reactive oxygen species (Anglada et al., 2009; Butkovskyi et al., 2014). Indirect or mediated oxidation has been shown to take place by reactive oxygen species such as •OH in the bulk solution (Butkovskyi et al., 2014; Panizza & Cerisola, 2009; W. Wu, Huang, et al., 2014). As reported based on

experimental evidence, hydroxyl radicals produced in the electrolytic process will non-selectively oxidize organic compounds more quickly than will other strong oxidants such as O_3 (Aieta et al., 1988; Anglada et al., 2009; Beltrán, 2003; Butkovskyi et al., 2014). This aggressive reactivity has benefits and risks because although it may helpfully oxidize persistent contaminants, the non-selective oxidation in the presence of salts may form halogenated by-products which may themselves be harmful contaminants. Halogenated by-product yield is one of the key disadvantages of the electrolytic process (Anglada et al., 2009; Butkovskyi et al., 2014), but is common among AOPs. However, other researchers have shown that by-products can be minimized by selection of the proper electrode material (Butkovskyi et al., 2014; W. Wu et al., 2014). Butkovskyi found that a combination of electrode materials, specifically ruthenium/iridium (Ru/Ir) mixed-metal oxide (MMO) anodes and titanium or silver cathodes gave optimal contaminant conversion to non-toxic compounds and the lowest production rate of undesirable by-products (Butkovskyi et al., 2014). Wu and co-workers discuss the advantages and disadvantages of a variety of mixed-metal oxide electrode materials for oxidation of pollutants where an anode's oxygen evolution potential (OEP) in terms of volts relative to a standard hydrogen electrode is a key measure of the anode's capability to efficiently oxidize pollutants in water. Although some mixed-metal oxide electrodes have higher OEP values than others, the practical application requires considering not only the potential for complete oxidation, but also the durability and corrosion resistance of the electrode and the operating current densities (W. Wu et al., 2014).

Electrochemical oxidation has been tested in laboratories using batch reactors as well as a flow-through design. The flow-through electrolytic reactor (FTER) moves contaminated water along a sequence of electrodes in a theoretical analog to groundwater flow behavior in the environment. Typical configuration of a flow-through reactor for treatment of polluted or waste water is with

the anode in the initial position so that the electrolyte has first contact with that active surface, maximizing contaminant degradation while minimizing cathodic precipitation of iron and carbonate species at higher pH (Gilbert, Sale, et al., 2010; Jasmann, Borch, et al., 2016).

Because groundwater generally flows, some investigation has been done into the application and effectiveness of an *in situ* reactive barrier system to treat recalcitrant compounds (Gilbert et al., 2010; Sale & Gilbert, 2002), with mixed results. The permeable reactive barrier (PRB) theoretically acts as a flow-through reactor, using the groundwater's natural hydraulic gradient as the driving force to move the contaminated water through the reactor's planar surface. Though the operation and maintenance costs were lower than standard pump-and-treat methods, the groundwater flow was not controlled to the extent that it was adequately retarded to ensure sufficient contact time between the contaminated groundwater and electrodes, and, by having a barrier in the path of the plume, back diffusion from low permeability zones downstream of the PRB may continue to contaminate the downstream groundwater. If the barrier is placed at the leading edge of the plume, the time horizon for all of the contaminants to arrive from the source can be too long to be practical.

The issues with *in situ* treatment are not altogether unique for electrochemical oxidation treatments, but must be considered as part of reactor design and treatment development. The environment at a contaminated site is very different from the environment in a laboratory, and the most effective scale-up work starts in the lab with an understanding of the issues present in the field, and with a vision of how those issues will be addressed.

2.3. Electrolytic treatment of dioxane

Electrochemical oxidation is being studied particularly for 1,4-dioxane because this is a treatment which by its nature is versatile, energy efficient, straightforward to automate, compatible with the environment, cost effective to use, and operationally effective to remove dioxane and other persistent organic pollutants (DiGuiseppi et al., 2016; Ghatak, 2014; Rajeshwar et al., 1994).

Lab-scale electrodes researched thus far for electrochemical oxidation of 1,4-dioxane are boron-doped diamond (BDD), and titanium-mixed metal oxide (Ti-MMO) tested with and without titanium-oxide (TiO_2) catalyst. Choi and co-workers (2010) studied the anodic oxidation of DX, comparing platinum-coated tin electrodes with BDD electrodes in a bench-scale stirred jacketed reactor. Results from this work showed a marked difference in degradation effective-ness between the two, with BDD electrodes giving 10x better reduction of chemical oxygen demand over reaction time. Choi and team also reported that running the temperature-controlled process at elevated temperature (55 ^{o}C versus 5 ^{o}C and 25 ^{o}C) resulted in faster DX degradation rates. BDD research done by Barndõk and co-workers focused on the nature of the electrolyte, comparing synthetic and industrial wastewater solutions and coupling a *Pseudomonas putida* biodegradation step with the electrochemical oxidation to test the biodegradability of the dioxane over the course of the electrochemical reaction (Barndõk, Hermosilla, et al., 2014). The Barndõk team's reactor design used BDD electrodes with recirculating flow and an air sparge to facilitate mass transfer, resulting in the key finding of the positive influence of elevated salt content in the dioxane solution with respect to total COD removal. Jasmann and co-workers furthered the work of Barndõk et al. by combining Ti-MMO electrode-based electrochemical oxidation with *Pseudonocardia dioxanivorans* biodegradation (Jasmann, Gedalanga, et al., 2017). Jasmann's selection of Ti-MMO electrodes for experimentation was based on three main factors:

1. The lower cost of Ti-MMO relative to BDD, which will be particularly important to capital cost considerations in large scale electrochemical reactor operations,
2. Ti-MMO electrodes have shown good resistance to fouling (through periodic polarity reversals), and
3. Ti-MMO electrodes have demonstrated degradation effectiveness as PRB components in field applications where chlorinated solvents and energetic compounds were mineralized *in situ* (Gilbert et al., 2010; Jasmann et al., 2016; Petersen, Sale, et al., 2007).

Additionally Jasmann and co-workers used Ti-MMO electrodes in combination with TiO_2 pellets in a flow-through electrochemical reactor in the dark, demonstrating that although TiO_2 is a known photocatalyst, it also performs as a catalyst without light (Jasmann et al., 2016). Jasmann et al. found that the presence of the TiO_2 catalyst in combination with electrolytic oxidation improved Ti-MMO degradation efficiency of DX by up to 460% over the electrolytic process alone, and that this was most marked in low ionic strength water. Their work also resulted in a proposed 1,4-dioxane degradation pathway showing that DX transforms in the presence of $^{\bullet}OH$ to open-ring products which are widely assumed to be readily biodegradable (Jasmann et al., 2016).

Knowledge gaps

Each of the studies by Choi, Barndõk, Jasmann and their co-workers used active mixing of the electrolyte, either through gas sparging, stirring, recirculation, or continuous flow through the reactor as a single pass. Static batch mode, with no imposed fluid movement, was not tested so it is unknown whether the electrolyte flow helps or hinders the DX degradation rate. Considering scale-up to field-scale deployment, a flow control system can be a unit operation in and of itself, adding to capital and operating costs, so it would be prudent to build a better understanding of the need for flow within an electrochemical reactor.

The BDD testing discussed here was done in reactors with no inter-electrode media present, but a similar set-up was not tested with Ti-MMO electrodes. The question of the impact of inter-electrode media on mass transfer within the electrochemical reactor is another key factor that may increase treatment efficiency, and thus will be important for field-scale application. Furthermore, if the reactor unit can be designed so that access to replace electrodes is straightforward, this will help ease the adoption of this technology as maintenance access issues can be minimized. Likewise having available a bench-scale testing unit, coupled with a pilot-scale testing unit would be very useful for gaining an understanding of a particular site's groundwater quality and performance with electrochemical oxidation because the reaction by-products, actual heat generation, and degradation reaction rate constants can be evaluated so that operating parameters including current density and treatment time to target can be determined.

None of the work discussed in this section has addressed the specifics of scaling up a test reactor to industrial scale or field installation size. However, based on work with Ti-MMO electrodes in a PRB used to target munition constituents in groundwater, Gent and co-workers suggest that a critical parameter for scale-up design is the reaction rate constant (Gent, Wani, et al., 2012). The reaction rate constant for a target contaminant degradation, whether the target is DX or some other compound, is dependent on the quality of the water at the impacted site. For the concept of a self-contained reactor, the reaction rate constant is important to understand for the purpose of reaction time required, other parameters like surface to volume ratio (important for heat transfer and for delivery of applied current density), and a relationship between salt content (solution conductivity) and effective current density may be more helpful.

Treated water in the DX experimental work discussed in this section was not analyzed for undesirable reaction products. Furthermore only one study looked at actual wastewater in addition

to the synthetic test solutions (Barndõk et al., 2014). Garcia-Segura and co-workers have reviewed several cases of electrochemical oxidation treatment of actual industrial effluents (Garcia-Segura, Ocon, et al., 2018), but these streams are different from groundwater because generally an industrial effluent stream can, or in some cases, must be characterized prior to outfall to meet environmental regulatory limits, so the reactor design could be based on the typical characterization, on the assumption that DX removal is required downstream of normal treatments. Groundwater in general is somewhat less predictable, when considering different sites and locations. In any case, designing the EAOP treatment to effectively remove the target contaminant(s) without forming unacceptable amounts of toxic byproducts is the goal.

3. BENCH-SCALE REACTOR CONFIGURATION TESTING

The objective of this part of the study was to test various operating modes using a bench-scale electrochemical reactor with parallel plate electrodes, and to design a pilot reactor based on these findings. Synthetic groundwater (SynGW) with known concentrations of contaminant and sodium chloride as the electrolyte was used for these experiments. The main parameter of interest across all modes was the degradation rate of 1,4-dioxane. The reactor was tested initially in batch mode to determine the DX degradation reaction rate kinetics, then was tested in continuous flow modes, with hydraulic retention time based on the previously determined reaction rate constant.

3.1. Materials

3.1.1. Chemicals

All chemicals were used as received: 1,4-dioxane (CAS 123-91-1) from Alfa Aesar, HPLC grade liquid, 99% minimum; sodium chloride (CAS 7647-14-5) from Fisher Scientific, certified ACS; dichloromethane (CAS 75-09-2), used for liquid-liquid extraction for gas chromatography - mass spectrometry (GC/MS) analysis, from EMD Chemicals, OmniSolv® High Purity Solvent liquid. Deionized water was produced on demand from a Barnstead Nanopure-Diamond™ deionized water system.

3.1.2. Construction materials

The undivided rectangular bench-scale electrolytic reactor was made of a sheet of Lexan™ (polycarbonate) cut and assembled to a rectangular shape using Gorilla Glue™ as the adhesive and a silicone sealant to seal all of the seams. The electrode frames were cut from a ¼-inch sheet of poly(methyl methacrylate) (PMMA or trade name Plexiglas®). Each frame is open in the center

along the path of flow, and is solid on three sides with a slit opening on the fourth side to allow the electrode to be easily slid into place, and likewise removed from the top.

Electrode frames were lined on the outside with a Viton round profile cord-stock gasket, cut to fit. The gasket made up for minor imperfections in the internal dimensions of the reactor. Gaskets were adhered to the frames with silicone sealant. This silicone sealant was also used to secure the gasketed frames in the reactor. Frames were installed so that their centerlines were 2.0 ± 0.1 cm apart, making the electrode centerlines also 2 cm apart. The edges of the frames were 1.5 cm apart, as indicated in Figure 2. The outlet port of the reactor was a tapped threaded opening fitted with a hollow-centered polyethylene screwed fitting that could accept a screwed plug or tubing.

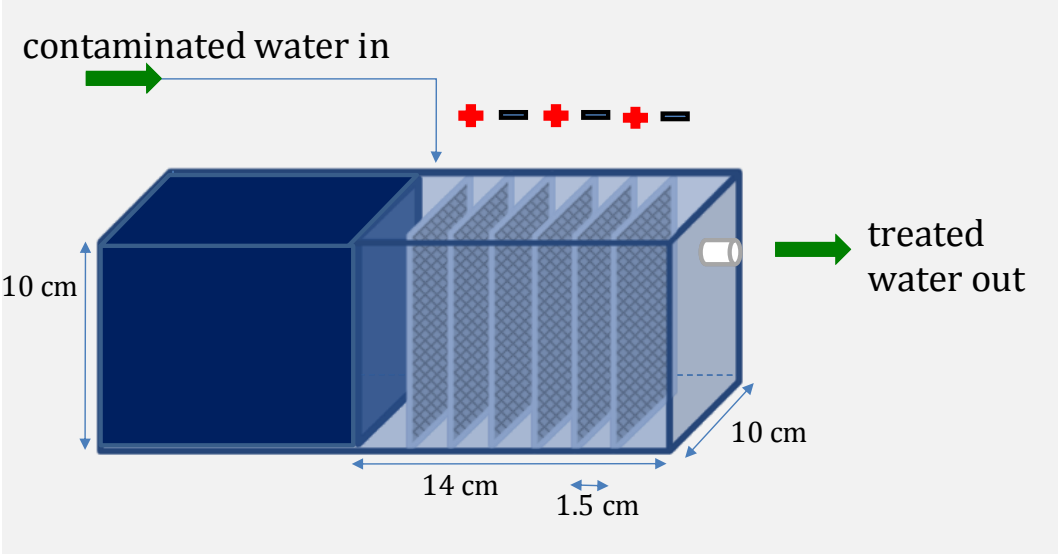

Figure 2 Bench-scale reactor diagram showing active chamber (with electrodes) and inactive chamber, at left, available for use in other configurations. The blank section in the middle can be repositioned to the left or right as needed to achieve desired reactor volume.

3.1.3. Electrodes and other materials

The electrodes used in this study (unless explicitly stated otherwise) were dimensionally stable expanded mesh Ti/IrO_2–Ta_2O_5 (Elgard^{TM}, 1.0 mm thick with 1.0 × 2.8 mm diamond-shaped

openings, Corrpro Companies, Inc., Medina, OH). These titanium mixed-metal-oxide (Ti-MMO) electrodes had large enough openings that solids-containing water would not clog up the system when run in flow-through mode. This material was used because of its relatively low cost (~ $400 m^{-2}), but more importantly because of its durability as both anode and cathode, and because it has been shown to be effective at mineralizing 1,4-dioxane without creating high amounts of undesirable reaction by-products (Chaplin, 2014; Jasmann et al., 2016; Radjenovic & Sedlak, 2015; Schaefer, Andaya, et al., 2015)

Solid soda lime glass beads, 6 mm in diameter, were obtained from the Colorado State University Chemistry Stockroom in one-pound lots. These were used as the inter-electrode media in the flow-through experiments.

The power to the system was supplied by a GW Instek® GPS-3030D bench-top direct-current (DC) power supply unit which itself was powered through a regular electrical outlet connection to the laboratory's standard 12 V / 120 A electrical circuit.

3.2. Methods

3.2.1. Solution preparation

Test solution was a synthetic groundwater (SynGW) made up of 1 g/L sodium chloride (NaCl) and 1 mg/L 1,4-dioxane in de-ionized (DI) water.

3.2.2. Bench- scale experimental set-up

The reactor was placed in a secondary containment tub in the laboratory fume hood. Electrodes were slid into the frames, with about 3 cm of electrode extending above the upper edge of the frames. A multi-patch plug was connected to the DC power supply's positive pole and another was connected to its negative pole. Three 18-gauge wires were connected to each multi-patch

plug, with the other ends connected directly to each individual electrode using alligator clips. This allowed alternating electrodes to be connected in parallel to the positive pole, making them the anodes, and the interspersed other electrodes to be connected in parallel to the negative pole of the power supply, making them the cathodes (Figure 2, above). Then the reactor was filled with synthetic groundwater until the electrodes were completely submerged.

3.2.3. Reactor operation

The DC power supply was set to constant current. Prior to applying power to the electrodes, the pH of the reactor solution was tested with a Denver Instruments pH meter, model UP-25, the temperature was measured with a spirit thermometer, and an initial solution sample was taken. Then the power supply, which was connected to a standard household 12V, 120A power outlet, was turned on. Regular periodic samples and parameter measurements were taken until the experimental treatment was complete.

Polarity reversal batch experiments in the bench-scale reactor were run just like the steady polarity experiments, except that a solenoid switch was connected to a common household electrical outlet timer between the power supply and the conductor connectors. The timer was set to alternate between off and on every thirty minutes. When the timer was "off" the polarity was unmodified, but when the timer was "on" the solenoid switch was closed and the polarity to the electrodes was switched.

3.2.3.1. Batch mode

Constant current at 3 amps, resulting in a potential of 8 V, was applied to the system for the batch mode experiments. Samples were taken at regular intervals. The current was applied continuously for the duration of each experiment. The completeness of the initial batch

experiments was based on GC/MS analytical results showing a reduction in 1,4-dioxane concentration of at least 50% of the initial concentration.

At the end of each experimental treatment period, the power was turned off and the reactor electrodes were disconnected from the power supply. The reactor and electrodes were rinsed with DI water from a spray bottle and the electrode positions were rotated, each one moving into the adjacent position, sequentially, to help prolong electrode life by running them alternately as cathode and as anode, and vice versa.

3.2.3.2. Continuous (flow-through) mode

Synthetic groundwater solution was added to a 22-L glass carboy. The carboy had been rinsed with DI water and left to air dry in the laboratory. The straight end of a hollow glass Pyrex tube was inserted into a length of polytetrafluoroethylene (PTFE) tubing. The other end, with a slight J curve, was lowered into the bottle. The tubing end was connected to a length of Viton 3-stop peristaltic pump tube for pumping from the feed vessel to the reactor. Downstream of the pump this feed line was connected to another length of PTFE tubing. The open end of this feed tube was fed through a 12 mm-diameter glass tube to a point at the anode end of the reactor. The large glass tube was supported by a ring stand and clamp so that it was stable and stationary. The feed tube itself was submerged to a central depth in the wetted area of the reactor. This set-up is shown Figure 3.

Figure 3 Set-up for bench-scale continuous flow (flow-through) experiments. Feed vessel in left rear, peristaltic pump in center, reactor at right.

A tube joint fitting was set into the port at the outlet of the reactor. The PTFE outlet tube was connected to a glass tee that served as an open leg to atmospheric pressure and as a siphon break. There were small quarter-turn valves at the atmospheric and downstream legs of the tee, for flow adjustment. The downstream leg of the tee was connected to a length of Viton 3-stop gear pump tubing. Both the feed and the outlet flows were driven by the same pump. Because of the vaporization of the reaction, the outlet flow had to be reduced slightly with respect to the feed flow to maintain a constant level in the reactor. This was achieved by the added restriction of a needle valve and an air gap to both control the flow rate out and to avoid siphoning the contents of the reactor out to the spent solution collection vessel, a 22-L glass carboy located on the floor outside of the laboratory fume hood.

The feed flow rate target was based on the half-life as determined in the batch experiments. Reaction time for degradation down to half the initial concentration ($t_{1/2}$) was about 10 hours, therefore, using a flow rate set point based on using the initial rate method, the continuous mode

was set up to allow for at least a 10-hour hydraulic residence time. The objective was to quantify kinetics before half the concentration was depleted, so the pore volume flow rate (PVF) was set at 1 PVF/12 hours. The theory was that this would be as close as possible to the actual hydraulic residence time in the batch experiments, and would furthermore allow adequate residence time to degrade more than 50% of the compound.

At start up, the outlet line was directed to the feed vessel and the pump turned on to allow the solution to recirculate without any power to the electrodes. Initial samples were taken only after recirculating the solution for two hours, to allow any sorption of 1,4-dioxane to surfaces and elastomers to take place before the establishment of an analytical baseline concentration for the solution in the system. After this recirculation period the outlet line was placed in the outlet receiver vessel and a sample was taken while the pump continued to run. After analyzing the pH of the grab sample (data shown in section 3.3 of this document) and taking aliquots for extraction in dichloromethane, the remaining solution from the sample was returned to the solution collection vessel. The temperature was not measured during this experiment because in the test set-up no temperature variation had been observed (data not shown).

When the continuous mode was tested with inter-electrode media present, the glass beads were added after the reactor had been emptied, rinsed with DI water, and allowed to air dry. The media had previously been rinsed twice with de-ionized water and spread out to dry on a layer of nylon mesh in a clean plastic tub in the laboratory fume hood. The dry beads were poured into the reactor with electrodes already in place, so that each inter-electrode gap was filled with the media to an equivalent depth. The pump speed was slowed from the no-media rate to maintain a similar solution residence time in the reactor.

DC power at 8 volts and 3 amps was applied to the system resulting in a current density of 11.0 mA/cm^2, normalized to anodic surface area. Power was applied continuously for the duration of each experimental treatment period. Samples were taken at regular intervals once the system reached steady state, as predicted by the half-life calculated from the batch experiments and based on preliminary sample analyses. The completeness of the treatment was based on GC/MS analytical results showing a reduction in 1,4-dioxane concentration of at least 50% of the initial concentration.

At the end of each experiment, the power was turned off and the reactor electrodes were disconnected from the power supply. The reactor and electrodes were rinsed with DI water from a squirt bottle and the electrode positions were rotated, each one moving into the adjacent position, sequentially, to help manage scale build-up and sustain reactivity by running them alternately as cathode and as anode, and vice versa.

3.2.4. Sampling and analysis

In batch mode, samples were taken at regular timed intervals via a 5000-µL pipette collecting 2 mL from each of the seven half-cell sections of the reactor. The 2-mL aliquots were mixed together in a 20-mL vial. Then 2 mL of that mixed sample were added to a 4-mL vial with 2 mL of dichloromethane (DCM) for liquid-liquid extraction for gas chromatography / mass spectrometry analysis (GC/MS). The remaining 18 mL of mixed sample was tested for pH then was poured back into the batch reactor between electrode #1 and the wall. In continuous mode, a sample from the outlet line at the waste collection vessel was collected in a clean 20-mL vial. Immediately after the sample was in the vial, 2 mL were pipetted out of the grab sample and added to 2 mL of DCM in a 4-mL screw-top vial for liquid-liquid extraction. The pH was measured in the 20-mL vial using a Denver Instruments pH meter. The excess sample was then disposed of

into the solution collection vessel. The DCM extract was transferred into a 2-mL amber gas chromatography (GC) vial with a septum screw top. The GC sample vials were stored in a local refrigerator at approximately 4 ^{o}C until analysis. GC/MS analysis for DX was done on an Agilent Technologies 6890N Network GC System with an Agilent 5973 Network Mass Selective Detector and a Hewlett Packard 7683 Series Injector, based on the major ion molecular weight of 88.1 ± 0.5 g/mol with elution time of 6.5 min., using a method developed by Jasmann and colleagues (Jasmann et al., 2016). Detection limits were determined at three times the standard deviation, S_o, for the results with a blank (Jasmann et al., 2016; USEPA, 2015).

The peak area of the initial sample is considered to be the starting concentration C_0 in each case, with subsequent peaks in a given experiment being the concentration C at a given time. The normalized concentrations (C/C_0) were plotted and evaluated with respect to time for each experimental period. The data was found to fit both the zero-order and first-order models based on linear regression ($R^2_{0\text{-}order}$ = 96.4%, and $R^2_{1st\text{-}order}$ = 97.0%), with good confidence in both cases ($p << 0.001$). The statistical evaluation output is in Table A1 in the Appendix. However, based on previous observations by other researchers it is generally accepted that electrochemical oxidation kinetics of aqueous organics at sub-mg/L concentrations follow a pseudo-first order model (Barndõk et al., 2014; S. Li, Bejan, et al., 2008).

After determining that reaction kinetics for DX degradation in SynGW follow a pseudo first-order model, additional data was evaluated based on that model. In each case the rate constant k was calculated using Equation 1 for batch mode, and using Equation 2 for continuous (flow-through) mode where k and k_{obs} = rate constant, t = reaction time, C = concentration at time t, C_0 = initial concentration, and HRT = hydraulic residence time (Jasmann et al., 2016).

Equation 1 Batch reaction rate constant

$$k = -\frac{\ln\left(C/C_0\right)}{t}$$

Equation 2 Continuous reaction rate constant

$$k_{obs} = -\frac{\ln\left(C/C_0\right)}{HRT}$$

In Equation 2 HRT represents the average time a compound in the flowing electrolyte remains in the reactive region in the reactor. The half-life, $t_{1/2}$, of a compound is the time it takes for concentration C to be 50% of the initial concentration so that $C/C_0 = 0.5$, expressed as Equation 3, where $t_{1/2}$ = half-life, and $k = k_{obs}$ = rate constant:

Equation 3 Half-life

$$t_{1/2} = -\frac{\ln(0.5)}{k}$$

3.3. Bench-Scale Reactor Results

Flow-through (continuous) degradation rates with and without inter-electrode media were compared in this reactor. Much of the DX electrochemical degradation testing done by others previously has found that degradation rates were mass-transfer limited, yet these studies were done with media present, based on the assumption that the media would aid in homogeneous flow distribution with respect to electrodes (Barndõk et al., 2014; Jasmann et al., 2016). The possibility exists, therefore, that mass transfer via bubble-driven convection is inhibited by the presence of media and low contaminant concentration. The degradation reaction rate constants and calculated $t_{1/2}$ results of the media / no media comparison are shown in the two bars at the left of Figure 4. When inter-electrode media was present $k = 0.036 \pm 0.002$ h^{-1}, but with no media the reaction rate constant nearly doubled, to $k = 0.071 \pm 0.004$ h^{-1}. These k values result in calculated half-life values of $t_{1/2}$ = 19 hours with inter-electrode media, and $t_{1/2}$ = 10 hours without media, suggesting that the

presence of media has substantial impact on mass transfer within the reactor, most likely by interfering with mixing.

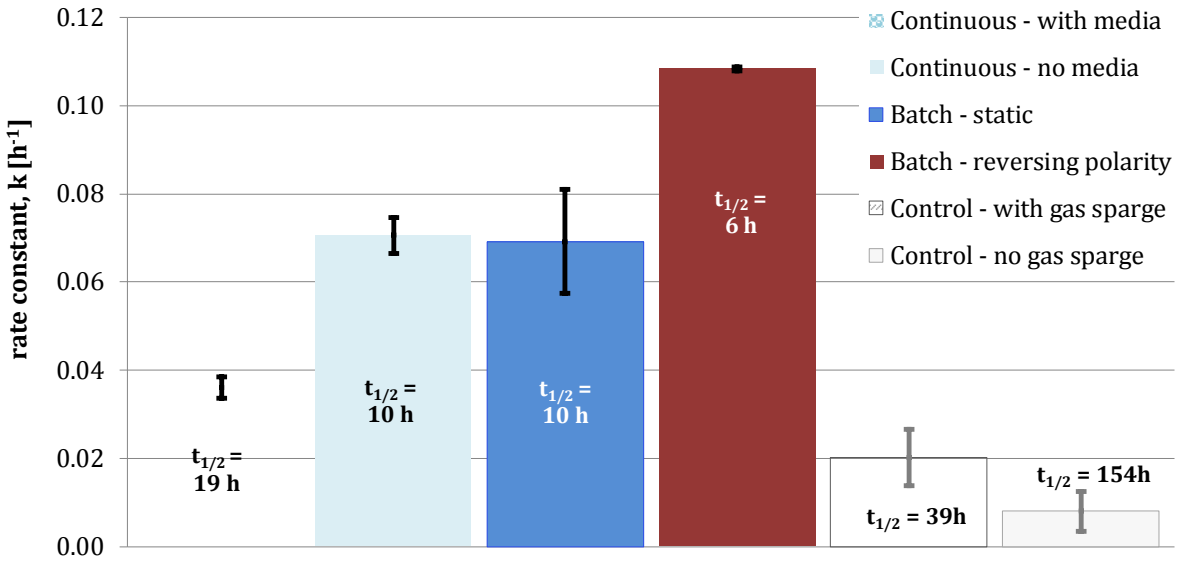

Figure 4 Bench-scale reactor 1,4-dioxane removal reaction rate constants for Ti-MMO electrodes. The presence of inter-electrode media does not improve reaction rate in continuous mode. Reversing polarity improves reaction rate by 40% compared to galvanostatic conditions in batch mode. Error bars shown are standard deviations based on number of replicates, n ≥ 3.

To further understand parameters that may affect the electrochemical oxidation rate, the reactor was tested without inter-electrode media, and without flow or recirculation, in a static batch mode. The results of the static batch mode experiments are represented by the third and fourth bars in Figure 5. When the reactor was operated in batch mode with constant polarity under galvanostatic conditions, similar to continuous mode, testing showed $k = 0.069 \pm 0.012$ h^{-1}, giving $t_{1/2} = 10$ h. A t-test revealed that there was no significant difference in DX removal between batch and continuous mode ($p = 0.351$, $\alpha = 0.05$). The static batch mode experiment was then modified to include periodically reversing the polarity. The fourth bar in Figure 4 shows that reversing polarity improves removal rate by 40% over batch constant polarity mode, with the reaction rate constant, $k = 0.108 \pm 0.001$ h^{-1}. This k value translates to $t_{1/2} = 6$ h.

The two bars on the far right in Figure 4 show results of control experiments where no current was applied to the electrodes as a test to determine if the detected change in DX concentration was wholly due to electrochemical oxidation, or if there might be some reduction in total DX due to other processes. For the control case wherein there was no sparge, meant to evaluate contributions to DX removal due to processes such as sorption, volatilization, photolysis or biodegradation, k = 0.008 ± 0.004 hr^{-1}, meaning $t_{1/2}$ = 154 h. When gas sparging was applied, the rate constant increased to k = 0.020 ± 0.006 h^{-1} ($t_{1/2}$ = 39 h), revealing the effect of gas-bubble induced DX stripping.

Normal configuration of flow-through multi-pair-electrode electrochemical reactors for oxidation of pollutants has the anode in the initial position, minimizing cathodic precipitation reactions (Gilbert & Sale, 2005; Jasmann et al., 2016). To test previous observations that having the anode in the initial position is important for the degradation efficiency of the reactor, a set of experiments was run with this anode-first configuration and another set of experiments was run with the cathode in the initial position. The results with no media are most pronounced, as shown by the tallest bar in Figure 5, where k = 0.071 ± 0.004 h^{-1} for the anode-first configuration. This is nearly 48% greater than the reaction rate constant for the equivalent no-media mode with the cathode first (k = 0.048 ± 0.004 h^{-1}). The presence of media had no positive impact on degradation performance when comparing anode first and cathode first, and when comparing against performance with no media, there was an apparent negative impact on the reaction rate.

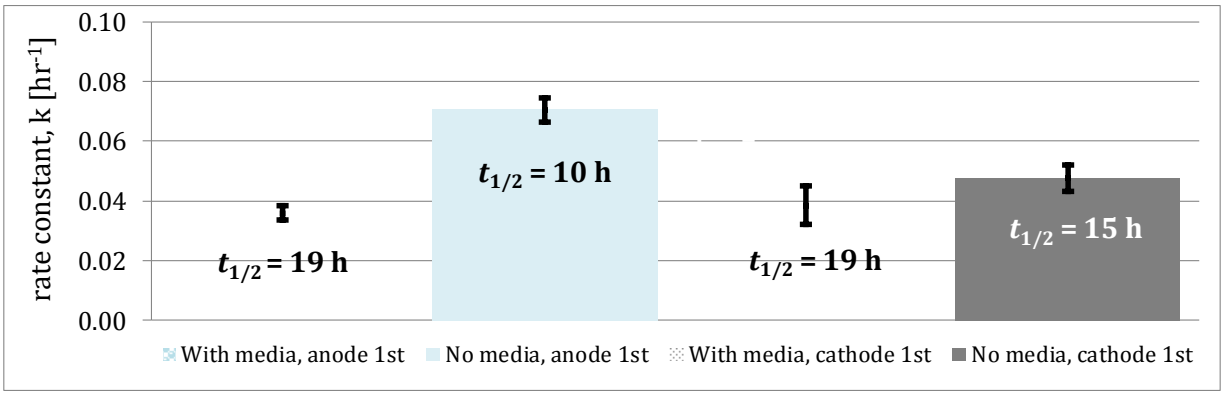

Figure 5 Dioxane degradation reaction rates and half-life values for the continuous modes tested in the batch reactor. n= 3 for each case.

3.4. Discussion of bench-scale reactor experimental results

The bench-scale reactor used in this testing is modifiable to a certain extent, in that the electrodes may be pulled out and replaced with fresh electrodes or electrodes of different material, and that electrode spacing may be changed. The experiments done for this study maintained a constant electrode spacing and varied other parameters, including flow rate, inter electrode media, and polarity. The batch mode operating concept is not novel in groundwater contaminant degradation research but most studies use an external reservoir or imposed agitation for the batch reaction (Barndõk et al., 2014; Choi, Lee, et al., 2010; Jasmann et al., 2016), so this is the starting point for the bench-scale reactor discussion.

Considering the degradation reaction rate constants for FTER operation with and without inter-electrode media, the faster degradation with no media present indicates that media may hinder mass transport. The glass beads in the reactor were in contact with the electrodes though there was interstitial space for direct contact of the electrolyte solution with the electrode surface. As the movement within the solution was impeded by media, in this case small spheres, there were more obstacles to good mixing between the bulk solution and the surface layer of the electrodes,

resulting in degradation reaction rate decreases as seen with $k = 0.036\ h^{-1}$ with media versus $k = 0.071\ h^{-1}$ without media. With no media present, there was less impediment to movement due to the pressure gradient in this system which was present in the form of bubbles and their physical movement through the solution, resulting in bubble-induced mixing (Petersen & Reardon, 2009; W. S. Wu & Rangaiah, 1993).

The next operational mode to consider is static batch mode without flow, recirculation, or mechanically induced agitation. The striking similarity in the reaction rate constant between FTER and batch mode reveals that mass transfer limitations in this reaction were not overcome by advection. In this batch system the Péclet number (*Pe*), which represents the mass transfer ratio of advection rate to diffusion rate, is much greater than 1 ($Pe \approx 2 \cdot 10^6$), indicating that advection rate dominates over diffusion rate. The Damköhler number (*Da*), which represents the ratio of reaction rate to diffusion rate, is also greater than 1 ($Da \approx 70$), indicating that electrochemical DX oxidation in this system is diffusion-limited. This supports findings by other researchers who report that, given adequate availability of reactive oxygen species, molecular diffusion is the dominant rate-controlling mechanism for contaminant degradation in FTERs including in plug-flow reactors, and for increased *k* values close to gas generation sites (Jasmann et al., 2016; Petersen & Reardon, 2009; W. S. Wu & Rangaiah, 1993). This latter relationship of gas generation sites, e.g. electrode surfaces, to increased *k* suggests that even without flow, the mixing engendered by gas generation may be adequate to incite enough intermolecular collisions for effective oxidation of the target contaminant.

Given effective degradation without flow, the next experimental step in this study imposed polarity reversals at 30-minute intervals. The reaction rate results of static polarity compared to polarity reversals ($k = 0.069\ h^{-1}$, and $k = 0.108\ h^{-1}$ respectively) is in line with the finding by Mena

and coworkers that there is a mixing effect created when a given electrode switches from an acting anode to an acting cathode (Mena, Villaseñor, et al., 2016). As discussed above, with molecular diffusion as the dominant rate-controlling mechanism, allowing for additional mixing without adding additional energy is an advantage of polarity switching. Ma and team built on the work of Röhrs and co-workers to find that polarity reversal repeatedly changed the direction of ion movement in the electrolyte as a result of the electrical double layer discharging or recharging as the electrode charge changes from positive to negative or vice versa (Ma, Wang, et al., 2010; Röhrs, Ludwig, et al., 2002). This change in the double layer leads to an increase in energy consumption, with shorter reversal intervals having higher energy consumption (Röhrs et al., 2002). But with optimal timing of the switching, particularly using longer rather than shorter intervals, the impact on overall energy consumption will be negligible compared with the benefit of increased reaction rates. Li and team reported the added benefit that polarity reversal, with its neutralization of excess H^+ and OH^- ions back to water molecules, helps to reduce the negative effect of OH^- when electrochemical oxidation is combined with a subsequent biodegradation step (T. Li, Wang, et al., 2016). Furthermore, polarity reversals are a critical part of long-term electrode maintenance to minimize scale buildup. Thus, the ability to perform regular polarity reversals without affecting treatment performance is another advantage of (non-directional) batch mode compared to continuous flow mode, in which the effect of polarity switching is likely to hinder rather than promote degradation due to periodically having a lead cathode (Gilbert & Sale, 2005).

Considering the comparison in continuous mode between lead anode and lead cathode, there was only a significant difference between the two when inter-electrode media was present (p = 0.043, α = 0.05). Without media, the lead-anode configuration resulted in about 30% shorter half-life than the lead-cathode configuration, confirming previous observations (Gilbert & Sale, 2005).

The control experiments were twofold: one was completely quiescent, with no flow and no power applied to the electrodes, while the other had nitrogen sparged into the reactor through a small ceramic sparger bulb placed on the bottom of the reactor. Both control experiments were each conducted for 10 hours like each of the other batch experiments, and all in the same open-top undivided rectangular reactor. The results for the sparged control indicated some amount of DX removal despite no applied potential. The quiescent control also showed some DX removal, but to a much lesser extent, and at a much slower rate than the sparged control. This leads to the conclusion that some portion of the DX decrease seen in this study to this point is due to gas bubble-induced stripping. Furthermore, the observed losses in the quiescent control imply further losses potentially due to sorption, volatilization, microbial action, or photolysis. However, losses due to photolysis are likely negligible because the DX is known to be a weak absorber of UV light, and the solution was not exposed to sources of light with the 185 nm wavelength to which DX is sensitive (Schuchmann & Von Sonntag, 1990; Stefan & Bolton, 1998). Given that the rate is low compared to the reaction rate with an applied potential, the other mechanisms may be considered to have a minor effect on the overall bench-scale reactor results.

4. PILOT-SCALE REACTOR DESIGN AND PERFORMANCE

The objective of this part of the study was to test a scaled-up version of the bench-scale electrochemical reactor using genuine contaminated site groundwater. The reactor was tested initially with SynGW to determine impacts of scale-up by evaluating the 1,4-dioxane degradation reaction rate kinetics, sample location impacts on dioxane degradation analytical results, and the actual temperature rise. An additional key objective was to quantify the formation of undesirable reaction by-products. Additional information on the SynGW testing can be found in the Appendix.

4.1. Materials

4.1.1. Chemicals

The chemicals used for testing the pilot-scale reactor with synthetic groundwater were the same as used for the bench-scale experiments (Section 3.1): 1 mg/L 1,4-dioxane in an electrolyte solution of 1 g/L NaCl in DI water. The DX-contaminated site groundwater (CGW) used was provided from an industrial site in the U.S.A. CGW was collected on 19 June 2017 and shipped on ice, overnight, to our laboratory in twenty 3.7-liter high-density polyethylene screw-top jugs. Sample jugs were stored in a laboratory refrigerator at 3 ± 1.4 ^{o}C.

4.1.2. Reactor materials and design

Based on the findings described above, the reactor was designed for batch mode operation. The body of the reactor was an off-the shelf high-temperature rectangular batch can, made of a single piece of polypropylene molded to 67.9 cm long at its rim by 37.5 cm wide by 34.3 cm deep. This type of batch can is typically used for food preparation and has a loose-fitting lid. Its two long sides were fitted internally with polyethylene sheets 1.3 cm thick that had been machined with

grooves 1.5 cm apart, as illustrated in Figure 6. These grooves served as guides for the electrodes, much like the frames that were used in the bench-scale design. The polyethylene sheets were each screwed onto the body of the reactor on the two longest vertical sides with six nylon screw-and-gasket sets for each sheet.

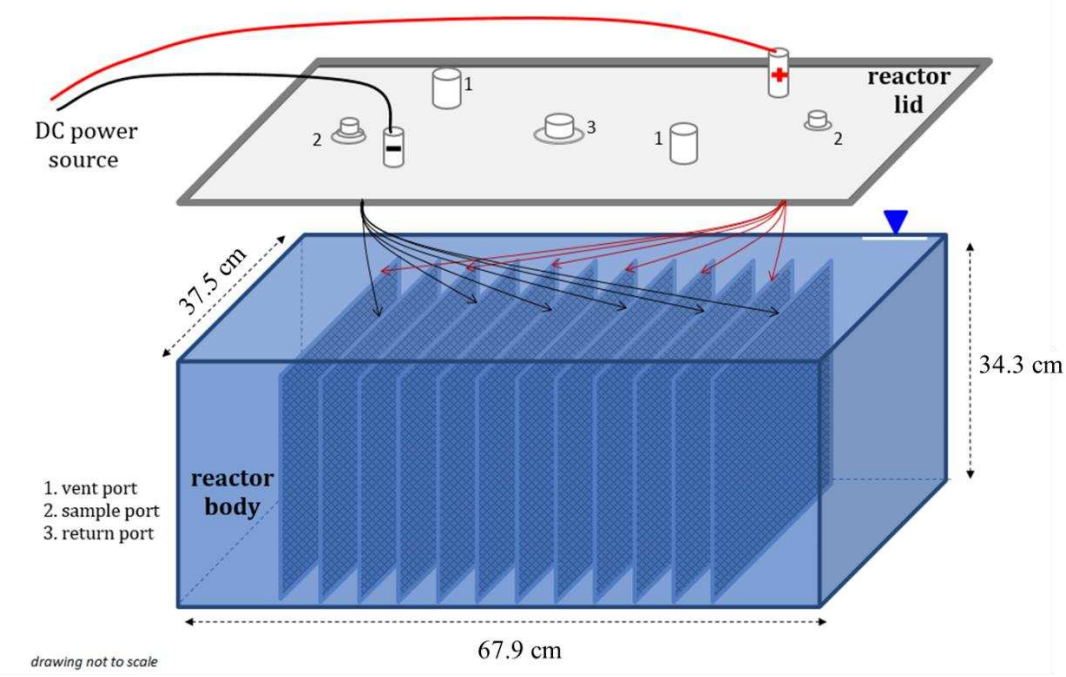

Figure 6 Pilot-scale reactor schematic showing the relative placement of the electrodes. Water fill level is at the top edge as marked at right by the triangle.

A synthetic rubber (ethylene propylene diene monomer, or EPDM) gasket was added to the top rim to help provide better sealing between the body and the lid, minimizing gas and condensate losses. Indoor/outdoor rubber weather-stripping was added to the inner edge of the lid to complete the seal and to guide any condensate drips from the lid directly back into the body of the reactor. Both gaskets and weather-stripping were adhered using the 100% silicone marine sealant used in the bench-scale reactor.

4.1.3. Electrodes

The same Ti-MMO expanded mesh electrodes were used in the pilot-scale experiments as in the bench-scale experiments. To facilitate even distribution of current across the whole of the electrode, distribution aids in the form of 1¼-cm wide, 0.09 cm thick titanium strips were spot-welded to each electrode about two inches in from a short edge as shown in Figure 7. The strip on each electrode extended from the edge of the electrode up past the opposite edge, making a tab about 7.6 cm long. A metal connector lug was spot-welded onto the end of the tab. All welds were cleaned with a wire brush then each connecter was crimped to the stripped end of a length of insulated 12 AWG stranded thermoplastic high heat-resistant nylon-coated (THHN) copper wire. The crimped connection was sealed in a double layer of heat shrink tubing, first to seal the connection between the wire and the crimped end of the lug connector, and second to seal the connection between the lug connector and the titanium distribution strip.

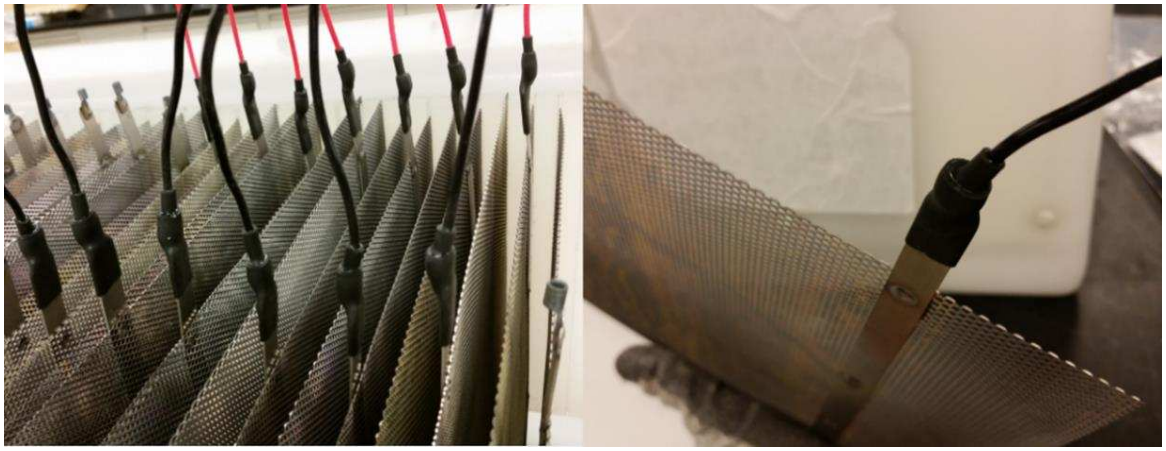

Figure 7 Pilot reactor electrodes in reactor at left, and out of the reactor at right. Visible are the spot-welded distribution strips and wiring connections.

The pilot reactor was designed to have a ratio of anode surface area to liquid electrolyte volume that was similar to the bench-scale reactor's anode surface to volume ratio of 0.17 cm^2/mL. For

this reason, the pilot reactor had 14 electrode pairs where the bench reactor had just three. The active (exposed) electrode surface area in this case was 24.1 cm x 29.2 cm per electrode, which gives a surface to volume ratio of 0.16 cm^2/mL.

4.1.4. Reactor power source

The power source for the pilot reactor was a cathodic protection rectifier made by Corrpower (Canada) for use in impressed-current cathodic protection applications in the field. This unit is powered by connecting to a standard 12 V / 120 A electrical outlet. Power adjustment is achieved by the use of 6-stop coarse and rough settings as shown in Figure 8. There is no independent control of voltage or current. The goal was to run the pilot reactor at the same or similar current density as was applied in the bench-scale reactor: about 11.0 mA per cm^2 of anode surface area.

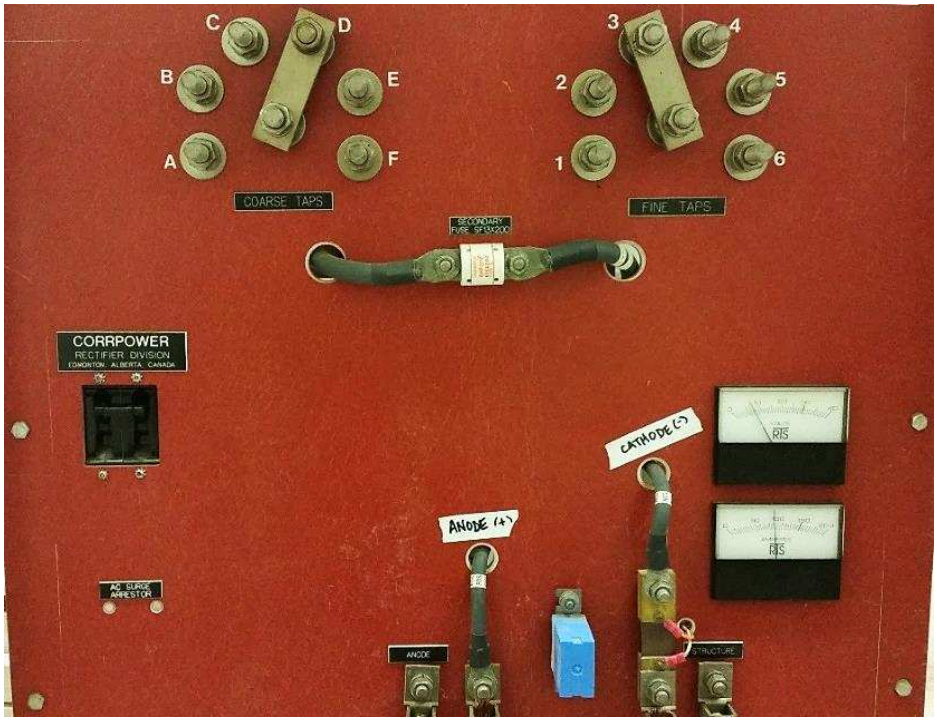

Figure 8 Rectifier face showing the 6-stop settings for coarse and fine power adjustment.

4.2. Methods

4.2.1. Solution preparation

Preparation of SynGW follows the same procedure as discussed for the bench-scale reactor (Section 3.2.1).

The contaminated site groundwater held visible solids, apparently fine sediment, which had settled to a layer 1 to 2 cm thick in the bottom of each of the sample jugs. Each sample container of site water was decanted to remove the bulk of these solids. Three levels of decant were tested by comparing DX recovery via GC/MS analysis before and after the decant. The three approaches were:

Level 1: simple pour-off of supernatant liquid,

Level 2: gravity filtration of the level 1 decant through laboratory grade filter media,

Level 3: gravity filtration of the level 1 decant through an off-the-shelf paper coffee filter.

The result of this testing was that level 1, the simple decant, was adequate to separate the majority of the solids from the liquid and to allow for recovery of the site-water dioxane. Each plastic one-gallon sample container was allowed to sit, letting solids settle after the container was carried by hand from the refrigerator in the workshop area of the lab to the chemical fume hood at the other end of the lab. After several hours the container was opened and the liquid was poured into a glass 4-L Erlenmeyer flask through a glass funnel. About 3.5 L was available for the initial decant of each 1-gallon container. As that volume was removed, the settled solids began to be stirred up and unsettled, so the remainder in the gallon container was poured into a 6-L round-bottom flask to settle further. Then the container was recapped, set aside, and the next container was opened. This was repeated until the total required volume had been decanted. The 6-L flask held several sample jugs' worth of final solids, which were allowed to settled out over 10 to 18 hours in the fume hood,

with the flask opening set at 90-degrees from vertical, to allow minimal solution movement while pouring, which allowed maximum recovery of low-solids supernatant. From the Erlenmeyer flask and from the round bottom flask, the decanted site water was poured into a 2-L graduated cylinder for volume measurement, then added to clean 20-L glass carboys for transport to the reaction laboratory.

4.2.2. Experimental set-up

The reactor, once assembled with the electrode guides in place, was wiped down with lint-free wipes, then rinsed with DI water. Then the 28 electrodes were installed into consecutive grooves, with 8.9 cm of open space at one end of the electrode cluster, and 10.2 cm of open space at the other end. The reactor with electrodes in place was then flushed twice with 4 liters of deionized water, and drained after each flush via siphon followed by physically tipping the reactor on its side to fully empty it. Then the connected electrode wires were bundled together and fed through nylon plastic submersible cord grips[1] in the lid of the reactor. The bundled wires, 14 each for anodes and 14 each for cathodes were joined in two separate copper #4 split bolt connectors with the stripped ends of two separate 2 AWG stranded wires, as pictured in Figure 9. The other ends of the 2-gauge wires were connected to the rectifier. All metallic connections were wrapped with electrical tape for safety.

[1] rubber bushing in contact with the insulated wires

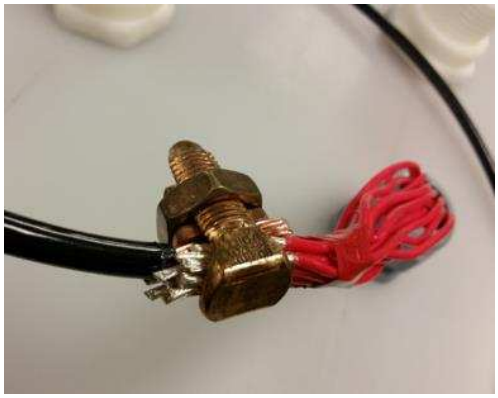

Figure 9 Exterior of reactor, 12-gauge wires joined with 2-gauge wires using split bolt connector, shown unwrapped. Cord grip is in untightened state

The reactor's power connections were tested initially by siphoning a salt-water solution (1 g/L NaCl in DI water) into the reactor until the electrodes were fully submerged. The rectifier was powered up and the reactor system was monitored for temperature increase and current fluctuations over the course of about three hours. The salt solution was then drained out, the wires unbundled, and the reactor well rinsed with DI water then drained and left to air dry with the lid ajar.

The reactor was placed on acrylic blocks in a large insulated open-top cooler box about 35 cm deep. The blocks were used to elevate the upper edge of the reactor above the edge of the cooler box. This box had 20-cm gaps at either end of the reactor and approximately 5-cm gaps on the sides, all of which were kept filled with ice water for the duration of the experimental period. The temperature of this water bath was monitored (data not shown).

With the lid off, the pilot reactor was filled via siphon through PTFE tubing from 20-L glass carboys. Because of the drop in head pressure in the carboy as it emptied, there was a loss of siphon pressure, so the last 4 L from each carboy was poured directly into the reactor. There was no level indication in this reactor, so it was filled to a premeasured volume, with visual confirmation to avoid overfilling and to ensure that all electrodes were well submerged.

4.2.3. Reactor operation

Once the CGW was loaded into the reactor the electrode wires were again bundled and connected to the larger cables connected to the rectifier leads. The rough and fine taps on the rectifier were set according to tested current delivered, and the system was powered up. Reactor parameters were monitored while the system was powered up. The two vent lines were directed into a laboratory fume hood and anchored in place on a tall ring stand to avoid creating a low spot in the line, which would have allowed condensing vapors to drip onto the fume hood surface. With the ring stand support, any coherent droplets inside the vent line would run back down the line into the reactor. The reactor was allowed to operate continuously, with exceptions for elevated temperature.

The reactor was run at two different current densities for this experiment. Initially operated at 9.5 mA/cm^2 to mimic conditions in the pilot reactor with SynGW, after 8.1 hours the system was powered down and left to rest overnight. Upon restart, the current was increased to achieve average current density of 12.5 mA/cm^2, where it ran for several hours until the current rose to nearly 130 A total, which was roughly the maximum safe operating limit for the system, resulting in a current density of 13.5 mA/cm^2. At that point the system was shut down for the night to allow the rectifier and the solution to cool down. Once cooled, the system was restarted at the same settings for an additional 7 hours, for a total of 16.6 hours at current density of 12.5 ± 0.6 mA/cm^2.

4.2.4. Sampling and analysis

Sampling location in the pilot-scale reactor was tested with SynGW by sampling from different locations in the reactor over the course of reaction time. Sampling locations are shown in Figure A2 in the Appendix. Results comparing normalized concentration over time indicate the sample location has negligible effect on measured concentration as shown in Figure A3 of the Appendix.

Based on this work, sample ports were installed in the lid of the reactor to allow the lid to stay closed, minimizing personnel exposure to harmful vapors, while allowing representative samples to be collected. Samples were taken using a 50-mL glass pipette, then transferring the solution into a rinsed, dry small Erlenmeyer flask. A combination pH and electrical conductivity (EC) probe was inserted into the flask for measurement of each sample. Once the measurements were recorded, the probe was removed, rinsed with DI water into a separate container, the contents of the flask were fed back into the reactor by the sample return port, and the flask was rinsed twice with DI water then inverted to dry. Temperature was measured in the reactor itself using a spirit thermometer which was able to reach down into the middle of the liquid volume. Analytical samples were pulled directly from the two reactor sample ports via 5-mL pipette and placed into separate vials for gas chromatography flame ionization detection headspace analysis (GC/FID), ion chromatography analysis (IC), and for liquid-liquid extraction with dichloromethane for GC/MS analysis. IC analysis was used to evaluate samples for chloride (Cl^-), chlorate (ClO_3^-), and perchlorate (ClO_4^-). These analyses were performed on a Dionex ICS-1500 ion chromatograph equipped with a Dionex IonPac AS16 analytical column (4×250 mm), using an injection volume of 100 µL. Detection and quantification limits for these anions are shown in Table 2.

Table 2 Analytical limits of quantification (LOQ) and limits of detection (LOD) for select chlorine ions.

	LOQ	LOD
Chloride, Cl^-	0.031 µmol/L (1.1 µg/L)	0.0092 µmol/L (0.33 µg/L)
Chlorate, ClO_3^-	0.033 µmol/L (2.7 µg/L)	0.0098 µmol/L (0.82 µg/L)
Perchlorate, ClO_4^-	0.040 µmol/L (4.0 µg/L)	0.0120 µmol/L (1.2 µg/L)

Initial GC/MS analysis was done on the contaminated site groundwater to determine the main contaminants present. Results of this analysis are shown in Table 3.

Table 3 Contaminant concentrations in CGW prior to decanting, and after electrolytic treatment in the pilot reactor. Units are µg/L.

Compound	Initial concentration, raw sample, pre-decant	Final concentration, pilot
chloroform LOQ = 113 µg/L, LOD = 34 µg/L	1310	28400
carbon tetrachloride LOQ = 131 µg/L, LOD = 39 µg/L	nd[1]	nd
benzene LOQ = 30 µg/L, LOD = 9 µg/L	265	nd
1,4-dioxane LOQ = 16 µg/L, LOD = 5 µg/L	626	44
chlorobenzene LOQ = 54 µg/L, LOD = 16 µg/L	115	nd
1,4-oxathiane LOQ = 144 µg/L, LOD = 43 µg/L	154	nd
chloropyridine[2] LOQ = 42 µg/L, LOD = 13 µg/L	100	97
dichloropyridine[3] LOQ = 86 µg/L, LOD = 26 µg/L	93	nd
bis(2-chloroisopropyl) ether LOQ = 206 µg/L, LOD = 62 µg/L	374	nd

[1] not detected [2] 2-chloropyridine [3] as 3,5-dichloropyridine

4.3. Pilot Reactor Results

Initial work was done with synthetic groundwater to test potential scale-up impacts from the bench-scale reactor, and to compare operating and DX degradation results with the known electrolyte. Following synthetic groundwater testing, the system was run with contaminated site

groundwater to study DX degradation rates, changes in certain co-contaminants concentrations, and the changing concentration of undesirable reaction by-products. In this section the main SynGW results are presented, followed by results for CGW.

Experimental results with SynGW showed differences from the bench-scale reactor in degradation reaction rate constant, half-life, and operational current density, as reported in Table 4. The rate constant in the pilot reactor is more than double that of the bench-scale reactor, with only a mildly elevated current density. Comparing the normalized log unit removal rate gives a clearer picture of the impact that current density may have on the degradation rate, with the bench-scale reactor (at constant polarity with no flow) reducing DX concentration by 583 $h*m^2/m^3$, versus 242 $h*m^2/m^3$ for the pilot reactor, as shown in Table 4. The normalized log unit reduction rate with respect to surface area is calculated using Equation 4 where ASA_{AO} is the apparent anode surface area per order, A = apparent anode surface area, V = volume of solution in reactor, $t_{0.1}$ = time to reduce the initial concentration by one order of magnitude, and k = rate constant. The lower the value of ASA_{AO}, the more efficient the process is per electrode area. More SynGW results are in the Appendix, Figure A5.

Equation 4 Apparent anode surface area per order removed (ASA_{AO})

$$ASA_{AO}\left[\frac{\mathrm{h*m^2}}{\mathrm{m^3}}\right] = \frac{A}{V} * \frac{\frac{\ln(10)}{k}}{\log\left({C_0}/{C}\right)} = \frac{A * t_{0.1}}{V * \log(10)}$$

Table 4 Comparison of bench-scale and pilot reactor current densities, and 1,4-dioxane degradation rate constants and half-life based on Equations 1 and 3, with ASA_{AO} based on Equation 4.

Ti-MMO electrodes only	**rate constant, k [h^{-1}]**	**half-life, $t_{1/2}$ [h]**	**current density [mA/cm^2]**	**ASA_{AO} [$h*m^2/m^3$]**
Bench (constant)	0.067	10.3	11.0	583
Pilot (SynGW)	0.150	4.6	10.6	242

With respect to the contaminated site groundwater, the initial concentration, C_0, in 59 L of CGW was 0.58 mg/L. While very little DX was removed in the first six hours of the low power period, Figure 10 shows that a total of 36% was removed by 8 hours at an average current density of 9.5 mA/cm^2. Dioxane concentration at the end of that period was 0.37 mg/L. In the idle period between the end of the low power period and the start of the higher power period the concentration decreased from 0.37 to 0.26 mg/L despite no power to the electrodes. The reason for this is unclear, but may be due to an error in sampling or analysis, though a similar drop from 0.11 to 0.08 mg/L occurred over the second shutdown period. In the second experimental period, when the electrodes were run at a higher current density, 83% of the dioxane still present in solution was removed, giving a final concentration of 0.04 mg/L after 16 hours at an average effective current density of 12.5 mA/cm^2. This is shown in Figure 11.

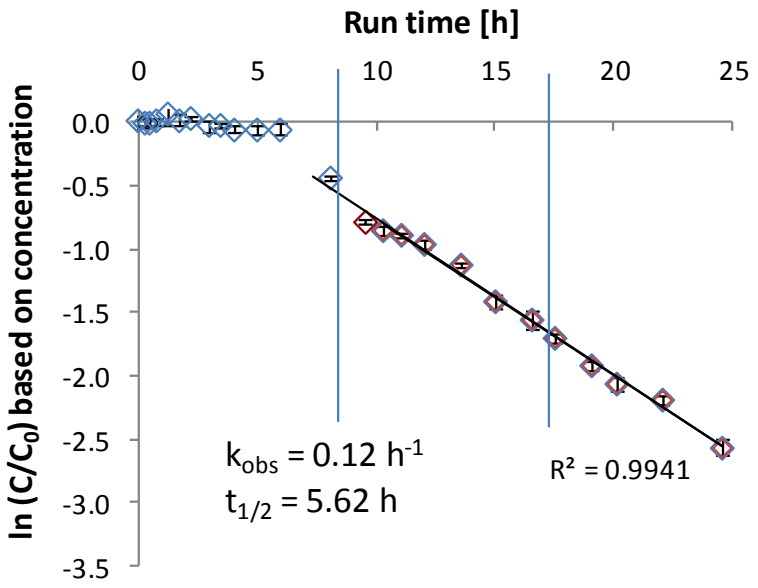

Figure 10 Pilot reactor reaction kinetics plot for contaminated site groundwater showing a pseudo first-order relationship for the degradation of 1,4-dioxane. The set of points with the flatter slope reflects operating at lower power with average current density of 9.5 mA/cm^2 (at 4 V, 95 A). The vertical line at 8 hours indicates a power shutdown. After that point the power was increased to deliver an average current density of 12.4 mA/cm^2 (at 4 V, 115 A). The second vertical line at about 17.5 hours indicates a power shutdown point with overnight hold.

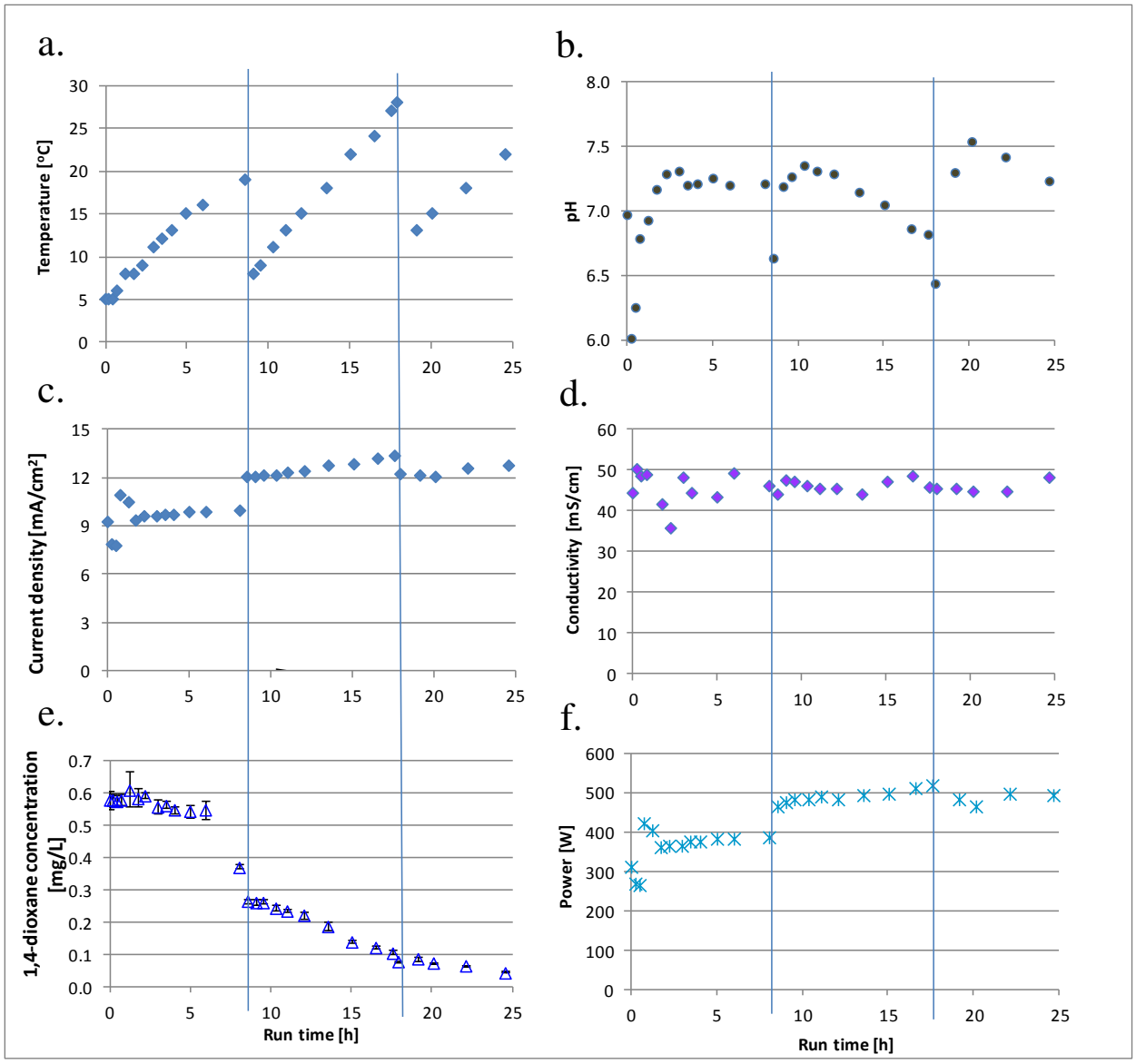

Figure 11 Pilot reactor data for contaminated site groundwater over total operational time. Vertical bars on the figure indicate power interruptions. Parameters are shown with respect to time: a.) Temperature, b.) pH, c.) Current density, d.) Electrical conductivity (EC), e.) 1,4-dioxane concentration, and f.) Total power.

Evaluation of CGW reaction kinetics during the period of higher current density reveals that DX degradation followed a pseudo first-order model as was also seen with the batch reactor SynGW results. Based on pseudo-first-order kinetics, the observed CGW dioxane degradation rate constant, k_{obs}, was 0.12 h^{-1} as shown in Figure 10. In this system, the DX half-life was 5.6 h,

from Equation 2. Overall 92% of 1,4-dioxane was removed from the contaminated site groundwater during the course of the total 25.7 h of electrochemical reaction time with Ti-MMO electrodes at a current density of 9.5 to 12.5 mA/cm^2. In absolute terms, 31 mg DX was removed. DX concentrations continued to decline until the end of the experiment to beyond the limit of quantification (16 µg/L), indicating that further reduction in concentration can be expected.

The plots of Figure 11, on the previous page, show select parameters across the duration of the electrochemical processing, including during the low power and high power periods. Power interruptions in reactor operation at 8.1 and 17.6 hours are indicated on the figure by the vertical lines. The temperature rose when power was turned on, and only stopped rising when the power was turned off. The saw-tooth temperature profile of Figure 11a is the result of running for a period of time, then powering down and allowing the electrolyte temperature to fall to below 15^{o}C. The bulk pH value showed a slight increase during electrolysis, but remained largely circumneutral, indicating a well-buffered water. The electrical conductivity was very high (44.3 mS/cm) for a groundwater sample and also remained largely constant, indicating relatively minor changes in the ionic strength of the solution, for instance via precipitation. As mentioned earlier the power was adjusted to deliver a higher current density; Figures 11c. and 11f. are analogous because the current density is calculated by dividing the current by the anode surface area to get current density in units of amps per area (A/cm^2). Similarly, power, in units of watts (W), is the product of current and voltage. Voltage stayed nearly constant, but at higher power, the current tended to increase over time, as did the temperature in both power modes.

Co-contaminants and disinfection byproducts (DPBs) of interest in this testing were tracked using GC/MS analysis based on an initial evaluation of the contaminated site water sample, and using IC analysis to quantify production of chlorate and perchlorate. Initial concentrations of the

organic compounds in the CGW are shown in Table 3, as the averaged results of triplicate samples analyzed by GC/MS prior to decant.

Concentrations of these compounds following processing are also presented in Table 3. Benzene and bis(2-chloroisopropyl)ether (b2CIE) concentrations decreased over the course of the reaction to below the detection limits. Neither tetrachloromethane (carbon tetrachloride) nor trichloromethane (chloroform) were detectable at the start of reaction. Carbon tetrachloride remained undetectable for the duration of the electrochemical reaction time, but chloroform was produced and its concentrations showed an increasing trend throughout the experiment, reaching a final average[2] concentration of 28 ± 3 mg/L as shown in Figure 12.

[2] The final set of triplicate samples each had one sample with a peak area of more than 20x the other samples for both chloroform and carbon tetrachloride. Including these data points gave a final average concentration of 246 +/- 308 mg/L. The likely outlier data points have been excluded in this reporting.

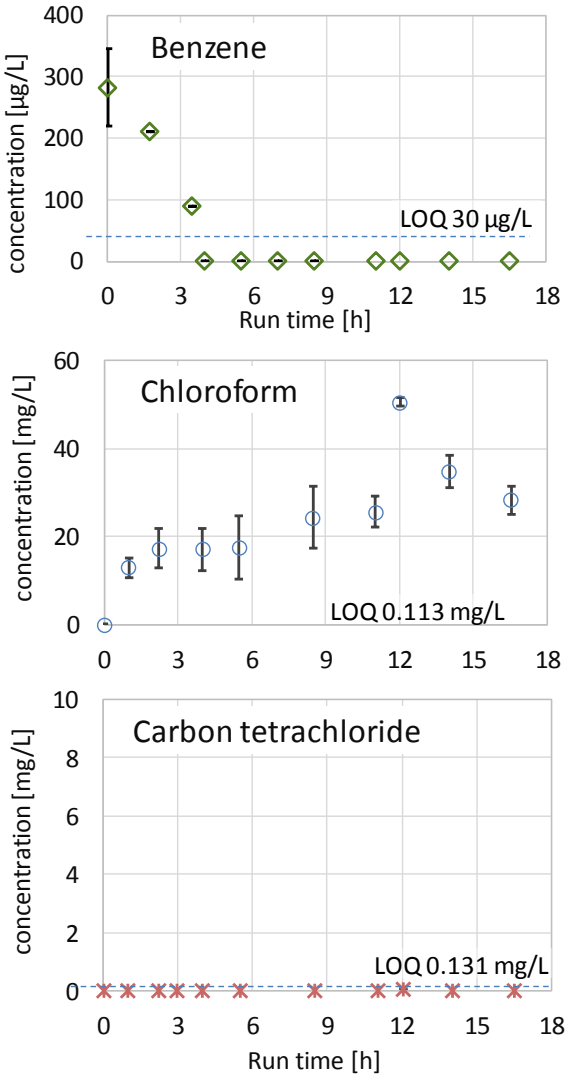

Figure 12 Change in by-product and co-contaminant concentrations in treated contaminated groundwater over time in the pilot reactor. n = 3 for each case.

IC analysis was used to evaluate processed CGW samples for Cl^-, ClO_3^-, and ClO_4^-, with results reported in Figure 13. The chloride concentration decreased by about 50 mM over 18 hours of reaction, and chlorate increased by about 50 mM. Perchlorate concentration stayed relatively low for the entire reaction time, increasing from below detection limits to 0.00084 mM by the end of the treatment period.

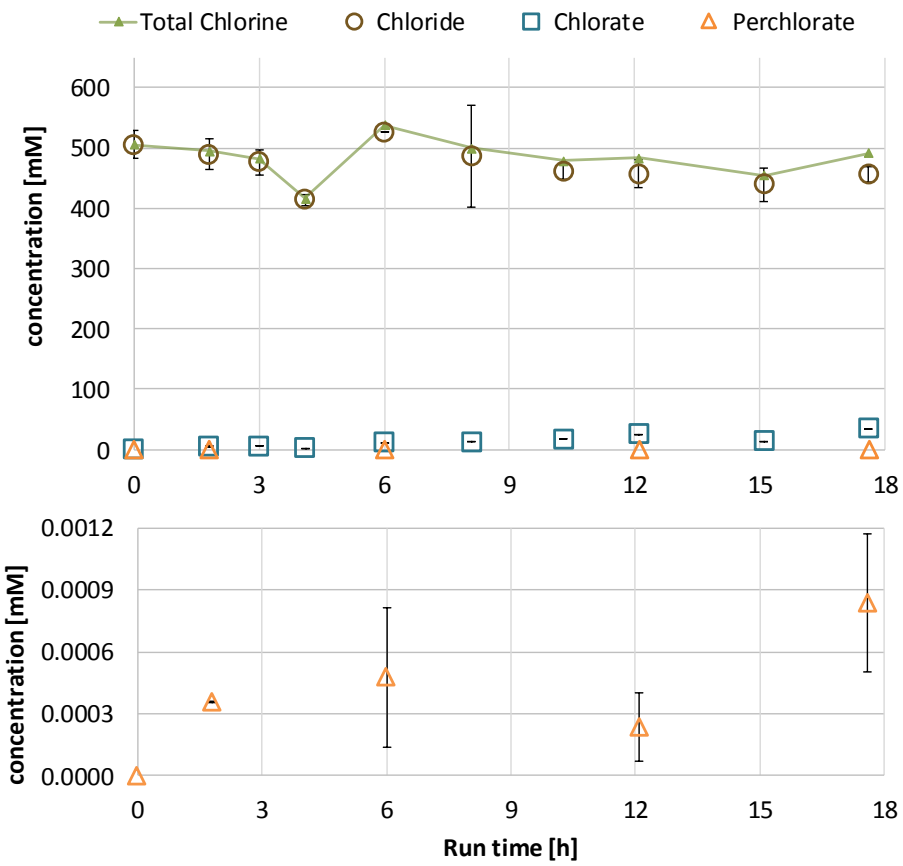

Figure 13 Change in chlorine ion concentrations in treated contaminated groundwater over time in the pilot reactor. Total chlorine includes moles of chlorine present in disinfection by-products chloroform and carbon tetrachloride. Bottom plot is zoomed in to a smaller scale, for clarity of perchlorate change. Where no data point is shown, the compound was not detectable. LOQ for all ≤ 0.04 µmol/L.

Reaction kinetics for SynGW in the pilot reactor are comparable to those for CGW, though the dioxane half-life in the former is shorter than in the actual site water. Table 5 compares reaction kinetics between bench-scale (SynGW with constant and reversing polarity) and pilot (SynGW and CGW, both with constant polarity).

Table 5 Comparison of bench-scale and pilot reactor 1,4-dioxane degradation rate constants with calculated half-life based on Equation 3. Bench-scale with reversing polarity is included here for comparison.

	rate constant, k [h^{-1}]	half-life, $t_{1/2}$ [h]
Bench (constant)	0.067	10.3
Bench (reversing)	0.108	6.4
Pilot (SynGW)	0.150	4.6
Pilot (CGW)	0.123	5.6

4.4. Discussion of pilot-scale reactor experimental results

The reaction kinetics for SynGW in the pilot reactor resulted in larger DX degradation reaction rate constants than in the bench-scale tests, although differences in current density were within only ±0.4 mA/cm^2. This indicates that the parameters of the current density and the ratio of electrode surface area to electrolyte volume are not the only parameters to consider in reactor scale-up and operation, and that other factors play a critical role in treatment efficiency. This is in contrast to statements by Chen, who claimed that current density alone "determines the rate" of the electrochemical oxidation process (Chen, 2004). The exact mechanisms behind the observed scale-up impact, however, remain to be determined. Similar to the bench-scale reactor, in this larger batch system, the Péclet and Damköhler numbers are much greater than 1 ($Pe \approx 2 \cdot 10^6$, $Da \approx 150$), indicating that electrochemical DX oxidation in this system is diffusion-limited. Da in this case is more than double that of the bench-scale Da because of the influence of the reaction rate constant in the relationship. The electrode spacing is the same in both cases, and the assumption has been made that the diffusion coefficient is constant across the two reactors, therefore it is the reaction rate constant which has the biggest impact in the difference between the pilot and bench Da values.

A key goal in the pilot reactor experiments was to maintain the same or at least similar current densities in the treatment of SynGW and CGW to allow for proper comparison of results. The nature of the system, however, allowed for only rough control of delivered power, so although current densities were similar, the applied electrical potentials were not: during the reaction periods of similar current densities, the system delivered an average of 6.3 V over the course of SynGW processing, and 4.0 V over the course of CGW processing (Figure 14). The potential was relatively steady in the two different cases; it was the current which markedly varied. Even at higher power, after about 8 hours the CGW potential remained steady, but the current increased by about 20 A, resulting in a current density increase of about 1.4 mA/cm^2 before the system was shut down due to high current load.

Nevertheless, the observed removal rate constants for DX were very similar with 0.150 h^{-1} for SynGW and 0.138 h^{-1} for CGW. It cannot be excluded, however, that this similarity is an artifact as previous studies have found the chemical composition of the water to have a major impact on degradation rates (Schaefer et al., 2015; Yan, Liu, et al., 2016; Zenker et al., 2003). Furthermore, several researchers have reported increased ·OH generation with increased current density, and it has been shown that increased ·OH production results in increased organic pollutant degradation rates (Costa, Montilla, et al., 2009; Kapałka, Fóti, et al., 2010; Martínez-Huitle & Rodrigo, 2015; Schaefer et al., 2015). The risk with increased current density and increased radical production is that more unwanted by-products will be generated as chlorine radicals are also generated and will non-selectively oxidize available compounds. Applied current density is determined by the power applied to the system, but functionally it also depends on the nature and concentration of the electrolytes.

Maintaining the target current density was challenging at the outset of the contaminated site groundwater testing because of the much higher salt content in the actual site water than had been tested with the SynGW. Most of the visible solids had been removed through the previously described decanting operations, but dissolved salts remained, substantially increasing the conductivity of the water. The contaminated industrial site water used in this experiment had conductivity of 44.3 mS/cm. For comparison, this conductivity is 100x the EC reported by the U.S. EPA for fish-supporting inland fresh waters (USEPA, 2012b). Conductivity of the SynGW was not measured but was calculated to be 2 mS/cm using the product of NaCl molar concentration (0.017 mol/L) and molar conductivity (116.5 cm^2S/mol) (Vanýsek, 2017). At similar current density (average 11.5 ± 0.9 mA/cm^2), the difference in conductivity between these waters is expressed as a higher potential during treatment of the SynGW (Figure 14), possibly explaining the somewhat higher rate observed in this test.

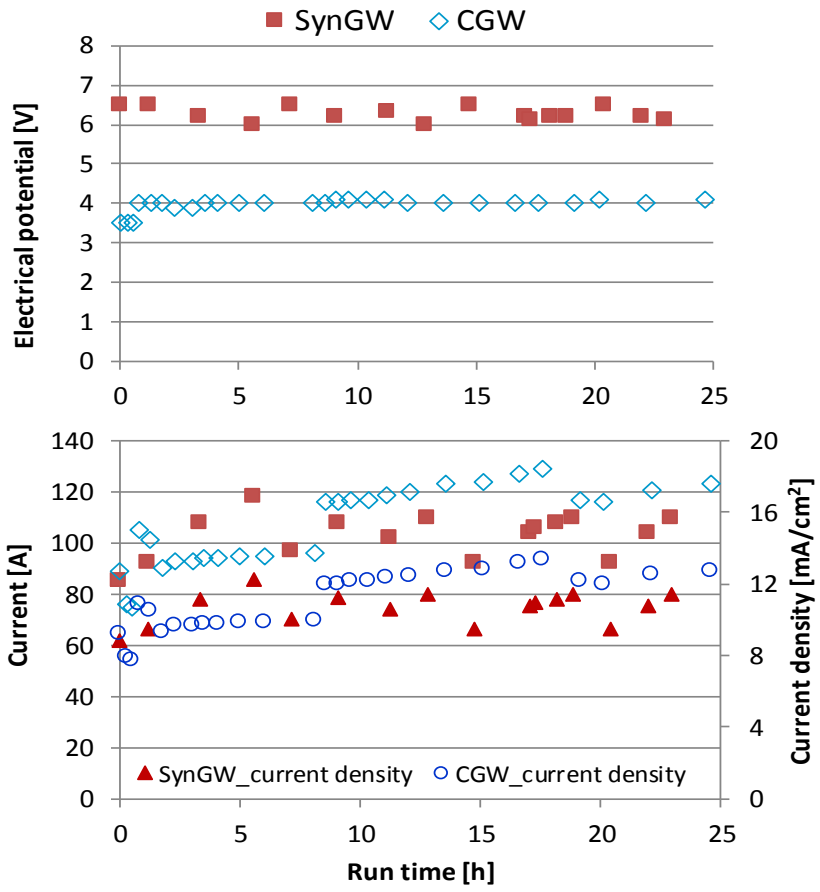

Figure 14 Ti-MMO electrode batch pilot reactor: comparison of potential, current, and current density between synthetic groundwater (SynGW) and contaminated site groundwater (CGW) processing.

The high salt content of the CGW allows for more reactions during electrolysis exposure than in the SynGW because more ions are available to compete for the hydroxyl radicals formed in the electrolyte solution (Bockris & Reddy, 1998; Yan et al., 2016; Zöllig, Remmele, et al., 2015). This may further explain the slightly longer DX half-life for CGW testing as shown in Table 5, above. However, beyond the competition aspect presented by the additional ions in the CGW, there are also likely to be compounds that act specifically as radical scavengers, reacting preferentially with hydroxyl and other radicals (Liao, Kang, et al., 2001). In groundwater, these scavengers include but are not limited to carbonates, bicarbonate, and organic materials (Aieta et al., 1988; Jasmann, 2016; Schmalz, Dittmar, et al., 2009).

The temperature in this reactor was managed passively with a water jacket around the reactor created by partial immersion in a non-circulating chilled water bath. Excess power input to the electrodes was transferred to the bulk reactor fluid as heat, and because the test solution was confined to the reactor with no active heat removal mechanism, the temperature in the reactor increased over time. Starting at a very low temperature helped to delay the onset of the temperature rise, but may also have had a detrimental effect on the reaction rate. Considering the temperature plot of Figure 11a. and the reaction kinetics in Figure 11c., the increase in temperature did not have a discernible impact on the reaction rate, which led to the conclusion that the reaction rate was not governed by rates of molecular collision as expressed through the classic Arrhenius equation for temperature dependence of a reaction (Equation A1 in the Appendix). In fact, the observed first-order kinetics imply that the reaction was mass transfer (S. Li et al., 2008). Yet it is interesting to note that mass transfer was apparently not enhanced by increasing temperature.

Organic contaminants often occur in mixtures at contaminated sites, possibly impacting each other's removal. As shown in Figure 12 above, the native co-contaminant benzene was removed over the course of the CGW experiment to below the limit of quantification, 30 μg/L. Benzene may have reacted with electrochemically generated radicals, or it may have been stripped to some extent by the energetic bubble formation at the electrodes. Previous reports quantified reductions in chemical oxygen demand in electrochemical treatment systems where both benzene and haloaromatics were present. Phenol and benzoquinone species were the most commonly detected intermediates from anodic oxidation of benzene (Kim, Kuppuswamy, et al., 2000; Oliveira, Salazar-Banda, et al., 2007; Santos, Dezotti, et al., 2013). Here, based on GC/MS analysis, no organic intermediates were detected.

It is known that some DBPs are generated during the course of AOP treatments, where the amount and nature of the by-products are determined by the quality of the water, including pH and (precursor) compounds initially present, the anode material, and the amount of applied current (Bagastyo, Radjenovic, et al., 2011; Rao, Somasekhar, et al., 2001; Schaefer et al., 2015; Zenker et al., 2003). DBPs in the form of chlorinated organics and inorganic oxidized chlorine species such as chlorate and perchlorate have previously been detected during electrochemical treatment and other advanced oxidation processes where 1,1,1-trichloroethane (TCA) and trichloroethene (TCE) are present as known co-contaminants with DX (Adamson, Newell, et al., 2017; Anderson et al., 2012; B. Li & Zhu, 2016; Sekar et al., 2016).

Organic DBPs are formed when organic precursor compounds react with oxidized chlorine species. Here, only chloroform was detected as organic DBP, although generation of other organochlorines such as dichloromethane is possible, partly explaining the incomplete chlorine mass balance (Zöllig et al., 2015).

This study targeted two main inorganic ionic compounds that are by-products of concern (chlorate and perchlorate) as well as their precursor, chloride. Perchlorate is a health hazard and is considered an emerging contaminant (Bergmann, Rollin, et al., 2009; Costa et al., 2009; Schaefer et al., 2015; Zöllig et al., 2015). The U.S. General Accounting Office reports several states have ClO_4^- advisory levels of 1 to 72 µg/L for groundwater, while the US EPA's office of Solid Waste and Emergency Response has recommended a preliminary remediation goal of 15 µg/L at Superfund sites (USEPA, 2017c). The starting chloride concentration in this pilot reactor study was 18.3 ± 0.8 g/L (505 ± 23 mmol/L). As the reaction progressed, the chloride concentration decreased gradually to a final 16.5 ± 0.1 g/L (456 ± 4 mmol/L). Chloride reacts with active oxygen (e.g. $^{\bullet}OH$) to produce chlorate. Chlorate likewise reacts with •OH to produce

perchlorate (Zöllig et al., 2015). The initial ClO_3^- and ClO_4^- concentrations in this study were effectively below the detection limits of 0.8 µg/L and 1.2 µg/L respectively. By the end of processing, the ClO_3^- concentration was 4390 ± 10 mg/L (52.6 ± 0.1 mmol/L) and the ClO_4^- was 84 ± 45 µg/L (0.0008 ± 0.0004 mmol/L). The roughly 50 mmol/L increase in chlorate is attributable to the roughly 50 mmol/L decrease in chloride as it oxidized to chlorate. The incomplete chlorine mass balance may be explained by generation of other species such as hypochlorous acid, (an intermediate in Cl^- oxidation to ClO_3^-), which was not analyzed in this study. A small amount of the chlorate further oxidized to form perchlorate. ClO_4^- generation is not surprising based on research by Bergmann and co-workers which has showed that ClO_4^- is produced during electrolytic oxidation of chloride-containing drinking water in a flow-through reactor (Bergmann et al., 2009). The final ClO_4^- concentration is in the range of maximum groundwater limits, at 45 µg/L, where groundwater recommended limits around the U.S.A. range from 1 to 72 µg/L. However, it has to be noted that the initial chloride (precursor) concentration in this groundwater was excessively high, and less perchlorate generation may be expected in more typical groundwaters.

Although the Bergmann study illustrated that ClO_4^- is produced at mixed-oxide electrodes, it concluded that boron-doped diamond anodes had the highest rate of ClO_4^- production by a factor of 10^3 over MMO and platinum anodes, which the work of Zöllig and team showed as well in their stirred batch reactor (Zöllig et al., 2015). Both studies conclude that higher current density in the electrochemical reactor may contribute to increased ClO_4^- production due to increased oxidant production. Using Ti-MMO electrodes at the lowest possible effective current density, as for example in a batch reactor with the ability to treat to target, may be an effective way to remove DX and to minimize the production of perchlorate. If perchlorate were generated at levels

exceeding regulatory limits, it could be readily reduced in a subsequent treatment step (Schaefer, Andaya, et al., 2017).

5. PERFORMANCE COMPARISON WITH COMMERCIAL TEST REACTOR

The objectives of this part of the study were to test a commercial bench-scale electrochemical reactor by quantifying the 1,4-dioxane removal rate and the formation of undesirable reaction by-products from contaminated site groundwater, and to compare results with the pilot-scale electrochemical reactor.

5.1. Materials

5.1.1. Chemicals

Contaminated site groundwater was used as described in section 4.1.1., above.

5.1.2. Reactor materials and design

The cylindrical plastic flow-through electrochemical reactor (FTER) was manufactured and provided by Magneli Materials, LLC, New Canaan, CT. It contains three sets of electrodes, providing a total of 396 cm^2 of apparent anode surface area. The three anodes are of a tubular form, with the stainless steel expanded-mesh cathode wrapped around the exterior of the anode. This is visible in Figure 16, below. Each anode is 14 cm long, with nominal diameter of 3 cm, for 132 cm^2 of apparent surface area per anode. The anode material is a Magnéli-phase titanium oxide (Ti_4O_7) in a ceramic membrane matrix on a titanium substrate. According to the manufacturer's specifications, the ceramic matrix is similar to, yet different from Ebonex® material. The anodes were coated with a stabilized Magnéli-phase titanium oxide for increased service life, rather than specifically for maximum oxidation rate. Figure 15 is an example of this anode.

Figure 15 Magneli Materials' tubular titanium-oxide ceramic membrane anode, excerpted from the vendor's website (www.magnelimaterials.com/industrial-water-treatment).

5.1.3. Reactor power source

The power source used was as described in section 4.2.4, above.

5.1.4. Pumps

Two Omegaflex model FPU5-MT positive displacement pumps were used to deliver the required flowrate. Platinum-cured silicone tubing was used with FBU500 tubing cassette on the pumps. These pumps were powered by standard 12V/120A electrical circuits. One pump was run at 320 rpm, and the other was run at 350 rpm to combined deliver about 2000 mL/minute, per manufacturer recommendation. The high flow rate is assumed to mitigate mass transfer limitations of the oxidation reaction at the anode surface.

5.2. Methods

5.2.1. Solution preparation

The contaminated site water was prepared for this experiment by simple decanting as described in section 4.2.1, to remove settled solids. The decanted solution was stored at room temperature following decanting.

5.2.2. Experimental set-up

The commercial reactor was set up on a small stand in the laboratory fume hood (Figure 16). DI water was recirculated for a period of time to flush the reactor. The reactor was connected to

the rectifier by two 4 AWG stranded wires. Then a sodium sulfate electrolyte solution was prepared, loaded into a six-liter round-bottom flask, and recirculated through the reactor as an additional surface flush and to allow for testing of electrical connections. The sulfate solution was drained out, then the unit was rinsed again with recirculated DI water, drained, and left in the fume hood overnight with all of its valves open to allow for draining and evaporation of residual water.

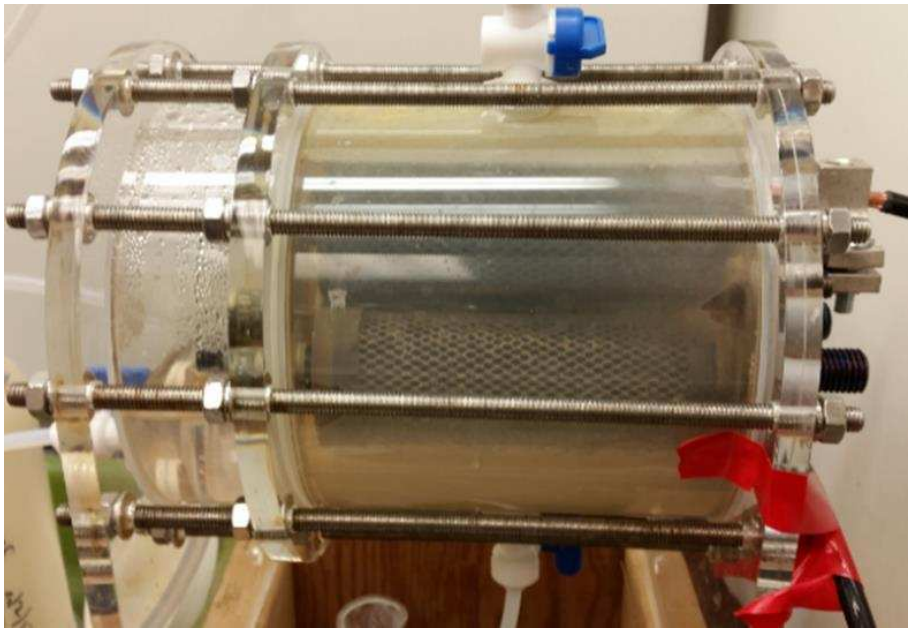

Figure 16 Commercial reactor with cathode mesh visible; anode is within the mesh. Feed chamber at left, vent on top, outlet on the bottom.

This FTER was designed to flow in from the bottom, allowing the electrolyte to contact the cathode surfaces first. The liquid within the electrode would pass radially in through the cathode to the anode, then travel down the anode annulus to the anode outlet chamber (at the left end of the reactor in Figure 16). However, based on initial experiments where there were gas build-up and venting issues, this study operated in the reverse, so that the electrolyte entered the unit from the side. This allowed the liquid to flow longitudinally initially through the annulus of the anode, then travel radially outward through the anode membrane and the expanded mesh of the cathode.

The outlet from the reactor was at the bottom. In all cases the vent line at the top allows generated gases to be released at a controlled rate. The liquid recirculates by flowing out through the bottom port back to the feed vessel. The vent line was directed to the feed vessel to allow liquid to flow freely through it.

5.2.3. Reactor operation

Once connections were made from the feed vessel to the reactor and secondary containment was in place, the pumps were powered up to allow the test solution to recirculate through the unit for a period of time before electricity was applied to the electrodes.

The system was shut down twice during the course of the experiment because of risk of overheating the system and potentially causing volatilization of DX due to higher temperature.

5.2.4. Sampling and analysis

Samples were taken from the feed/recirculation vessel using a 5000-µL pipette with plastic disposable tips. The samples were placed directly into vials for ion chromatography analysis or for liquid-liquid extraction with dichloromethane for GC/MS analysis. A combination probe to measure temperature, pH, and electrical conductivity was inserted into the recirculation vessel for readings when analytical samples were taken. This probe automatically temperature-adjusts the EC and pH values reported. Once the measurements were recorded, the probe was removed, wiped down, and rinsed with DI water into a separate container.

To evaluate the impact of DX volatilization on total removal rate, a Tedlar® bag was attached to the vent outlet hose to collect a vapor sample when the recirculating solution temperature got to 50 °C. The sample was collected by allowing the vent line tubing to empty of liquid, then frequently and periodically opening the vent valve the smallest amount possible to collect vent gas

while minimizing the collection of liquid into the bag. In the 25-minute sample collection period, reactor vapors were collected along with several milliliters of solution. After collection, the bag was immersed in water to measure the volume of gas based on the water displacement. The gas was extracted into *n*-octanol for later GC/MS analysis.

Quantification and detection limits are listed in Table 2 in section 4.2.4.

5.3. Results with contaminated site groundwater (CGW) in the commercial reactor

Reaction kinetics for the CGW indicate 1,4-dioxane degradation again followed a pseudo first-order model as was seen with the other reactors in this study. Based on the pseudo first-order model, the observed DX degradation reaction rate constant, k_{obs}, is 0.944 h^{-1} as shown in Figure 17, following an initial lag phase that showed a very slow rate of change. The k_{obs} for the lag phase was 0.217 h^{-1}. The duration of the lag phase was about 1 hour. At a flow rate of 2 L/min, this means there were roughly 60 turn-overs of the reactor contents before the reaction rate increased to the level seen for the remaining 3.5 hours of processing. There is a lag seen in all cases from the initial DX concentration to a point in time when the concentration begins to decrease. This happened in all start-up and restart cases following a shutdown of more than a few minutes. This phenomenon bears investigation, particularly as the design moves into scale-up. Schmalz and co-workers identified a lag phase of about 8 minutes over a 60-minute reaction period in electrochemical disinfection of wastewater with BDD electrodes, where the pseudo first-order kinetic relationship did not become evident until after a period of time. Their interpretation is that this lag was due to the competitive consumption of the generated oxidants by other wastewater compounds interfering with the steady degradation of the target species (Schmalz et al., 2009). Schaefer and co-workers also report a lag of 0 to 40 minutes over a 120-minute reaction period in

the disinfection rate in their study of by-product formation from electrochemical treatment of surface water with Ti-MMO electrodes, though they report that the lag time decreased with increasing current density (Schaefer et al., 2015). Neither study delved more deeply into the cause of the lag (Schaefer et al., 2015; Schmalz et al., 2009). The lag phase may be attributable to competitive reactions, but because it was not a phenomenon isolated to initial start-up, it could also be due to some interactions involved with the formation or dissipation of the gas bubble layer on the electrode surface. This study did not further investigate the cause of the lag.

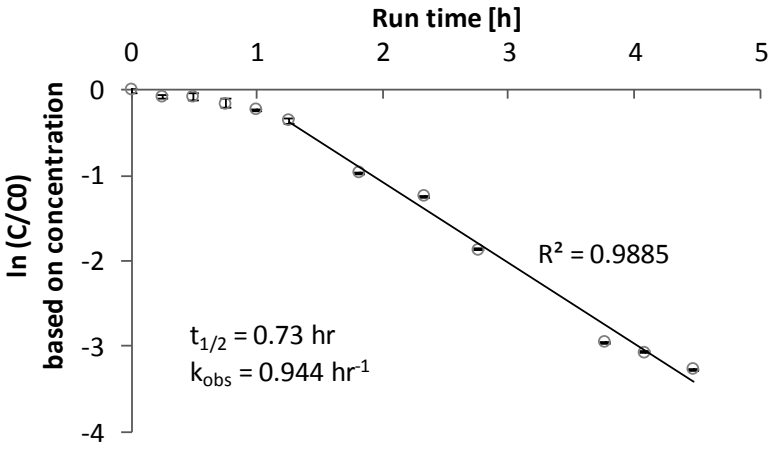

Figure 17 Commercial reactor reaction kinetics plot for contaminated site groundwater showing a pseudo first-order relationship for the degradation of 1,4-dioxane.

In this system the DX half-life ($t_{1/2}$) was 0.73 h (Equation 3). Overall 97% of DX was removed from the contaminated site groundwater during the total 5 hours of electrochemical reaction time in the recirculated reactor with Magnéli-phase titanium ceramic membrane anodes at a current density of 115 to 131 mA/cm^2. In absolute terms, 2.1 mg DX was removed. As mentioned at the end of section 5.2.3., the gas was collected from the vent line for a period of time during the CGW treatment. The extraction of the collected gases into octanol yielded 0.023 µg/L DX (assuming that extraction was 100% efficient), which, based on the 26-minute collection time gives a rate of

vaporization of about 0.591 µg/h. This means that approximately 3 µg of DX was lost to volatilization. The initial concentration, C_0, in 3.5 L of CGW was 0.620 mg/L. DX concentration at the end of processing was 0.024 mg/L. The plots of Figure 18 show select parameters across the duration of the electrochemical processing. Power interruptions in reactor operation at about 1.3 and 2.8 hours are roughly indicated on the figure by the vertical lines. The temperature rose at the beginning of the experiment and stayed elevated for the duration of the electrolytic reaction time. Aside from an initial elevated pH followed by a brief decline as the temperature rose, the pH stayed relatively circumneutral after one hour, at about 7.0 ± 0.3. Solution conductivity increased only after an initial lag phase of little to no change, then a roughly 70% increase from the starting conductivity. 1,4-dioxane concentration likewise decreased after an initial but more abbreviated lag period.

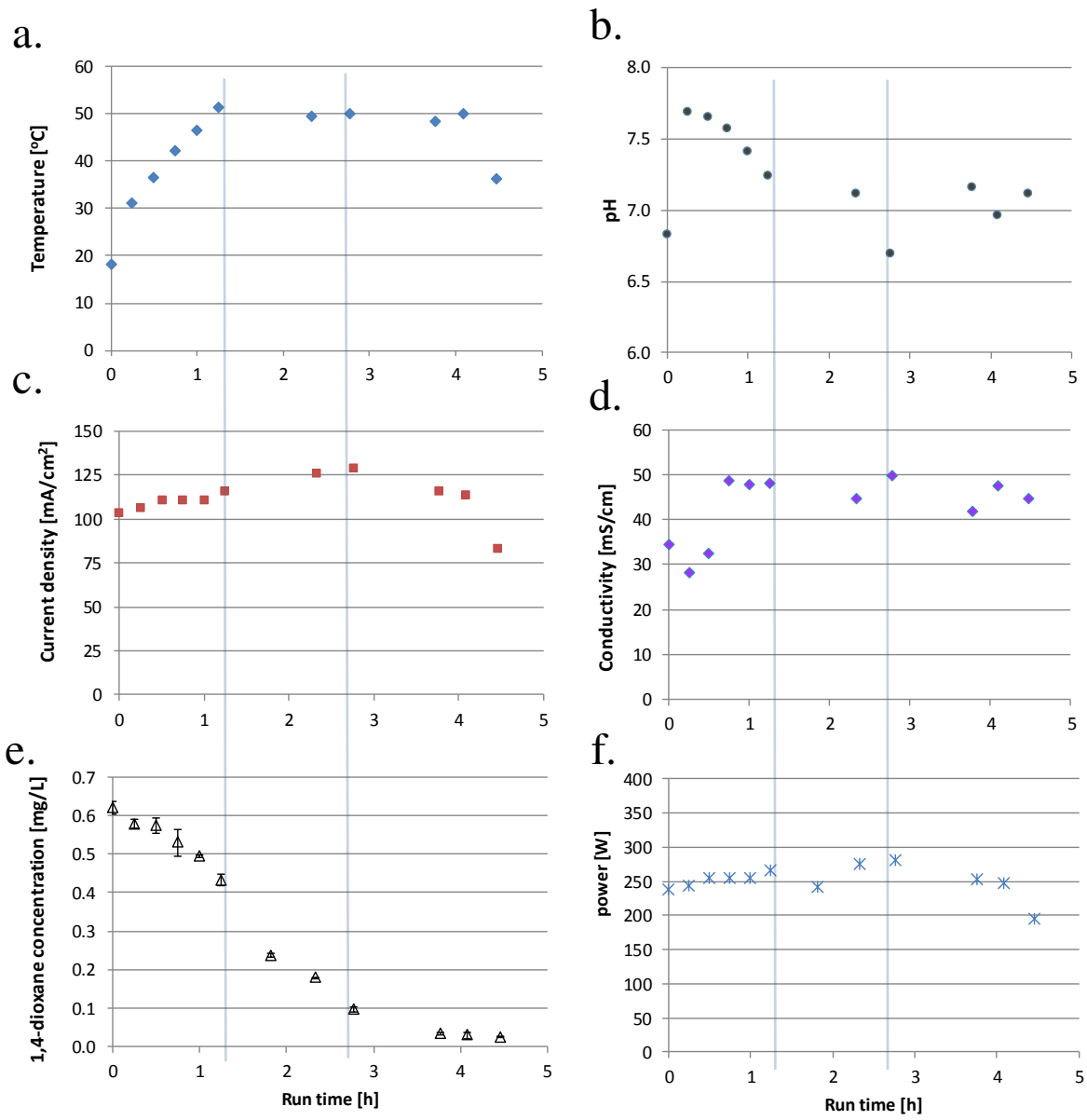

Figure 18 Commercial reactor reaction over the total operational time. Vertical bars indicate power interruptions. Parameters are shown with respect to time: a.) Temperature, b.) pH, c.) Current density, d.) Electrical conductivity, e.) 1,4-dioxane concentration, and f.) Total power.

Some co-contaminants and reaction by-products of concern were tracked using GC/MS analysis, with results shown in Figure 19. Benzene concentration was > 100 µg/L at the start of processing, but decreased to below the detection limit of 9 µg/L within 2.5 hours. At the start of processing, chloroform and carbon tetrachloride were below detection limits (34 and 39 µg/L

respectively), but their concentrations increased during processing to 27 ± 4 mg/L ($CHCl_3$) and 4790 ± 75 µg/L (CCl_4).

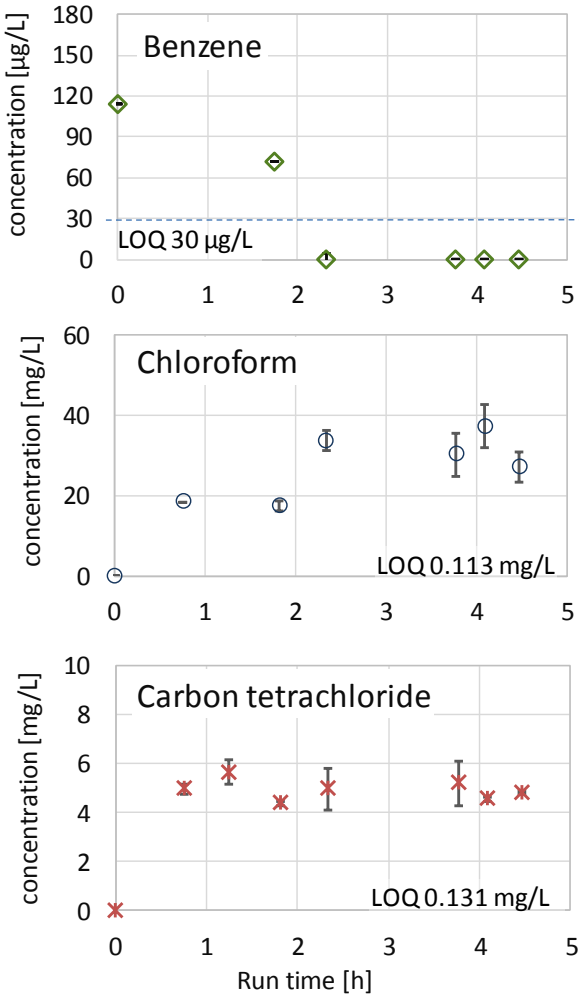

Figure 19 Change in by-product and co-contaminant concentrations in treated CGW over time in the commercial reactor.

As presented in section 4.3., this study used IC analysis to evaluate samples for chloride, chlorate, and perchlorate. Figure 20 shows the changing concentrations of these ions over time. Chloride concentration decreased by about 220 mM over 5 hours of reaction, while chlorate increased from below the limit of detection to about 200 mM. Perchlorate concentration increased from below the limit of detection to about 0.15 mM at the end of processing.

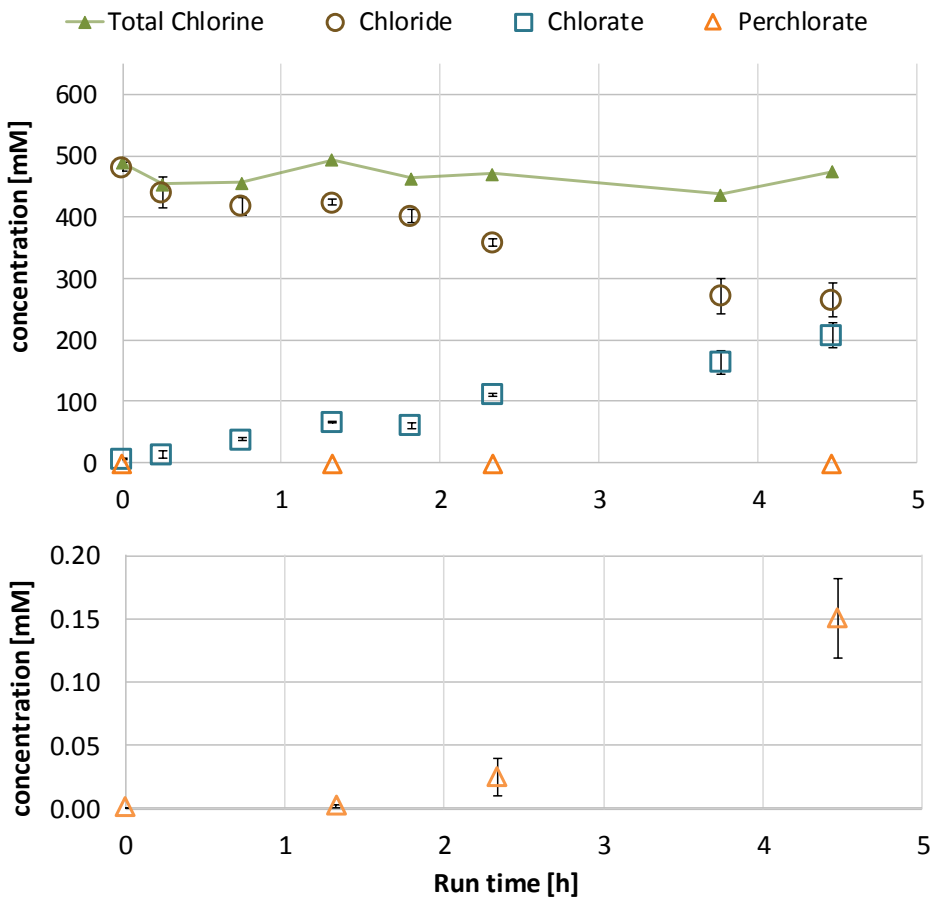

Figure 20 Change in chlorine ion concentrations in treated CGW over time in the commercial reactor. Total chlorine includes moles of chlorine present in disinfection by-products chloroform and carbon tetrachloride. Where no data point is shown, the compound was not detected. Bottom plot is zoomed in to a smaller scale, for clarity of perchlorate change. LOQ for all ≤ 0.04 µmol.

5.4. Discussion of commercial results and comparison with pilot-scale results

As mentioned earlier, a key goal in the pilot reactor experiments was to maintain the same or at least similar current densities in the bench- and pilot-scale reactors. This goal of current density of about 11 mA/cm^2 also applied to the operation of the commercial Magnéli-phase titanium ceramic-membrane anode reactor, but with the different electrode materials and the electrode bundle design, with its relatively small surface area (396 cm^2) compared to the anode surface area of the pilot reactor (9650 cm^2), it was not possible to achieve a current density below 100 mA/cm^2

for any sustained length of time. In the initial set-up and testing of this reactor, the operational recommendations of the manufacturer were followed, so it was a voltage target rather than a current target that was the operational set point, though the control capabilities allowed by the cathodic protection rectifier did not allow for a selection of type of control. Nevertheless, the system was adjusted such that the recommended voltage of 6 ± 0.5 V was maintained. The delivered current was in the range generally from 41 to 50 A, which delivered the very high current density range of 100 to 130 mA/cm^2 for the majority of the commercial reactor operation.

Temperature rise in this reactor was managed by shutting down the rectifier and then the pumps when the solution temperature reached about 50 ^oC, then letting the system sit idle until the solution cooled back down to approximately 20 ^oC, then the system was restarted again. The volume of test solution in this reactor was a fraction of the volume in the pilot reactor, resulting in less of a heat sink, and allowing for a rapid temperature increase, from 18 ^oC to 52 ^oC in the first 1.3 hours. The main concern with unchecked temperature rise was the potential for thermally driven mechanisms such as volatilization to play a part in the removal of 1,4-dioxane, blurring the effects of oxidation reactions due to electrolysis.

Reaction kinetics for DX removal in the commercial reactor show fast reaction time, with an observed reaction rate constant nearly six times that of the pilot reactor with CGW. However, the applied potential, the current density, and the ratio of electrolyte volume to electrode surface area were different between these two experiments. The commercial reactor was operated with a relatively small volume of solution and used mechanical recirculation to force the solution through the electrodes, while the pilot reactor was operated with roughly twenty times the volume, with no external mixing or applied recirculation. The movement of the fluid within the pilot reactor was due only to the movement generated by the evolution of gasses during the electrolysis process. Yet

pseudo first-order kinetics indicated that reactions were mass transfer-limited in both cases (S. Li et al., 2008).

The tubular ceramic membrane anodes in the commercial reactor have a multitude of tiny pores of unspecified dimension, resulting in a much greater effective surface area than the calculated apparent surface area considered in this study for current density comparisons. The expanded mesh sheets of the Ti-MMO electrodes likely also have more effective surface area than the apparent surface area which was calculated based on the electrodes' planar two-dimensional area. Yet the specific surface area in both cases is not known, so surface area-based values (e.g. current density) must be considered to be approximations rather than absolute values. For a normalized comparison of these two reactor systems, the log unit removal rate was calculated according to Equation 4 (Section 4.3), and a power-normalized comparison was done based on Equation 5 (Radjenovic & Sedlak, 2015).

Equation 5 Electrical energy per order (E_{EO})

$$E_{EO}\left[\frac{\text{kW h}}{\text{m}^3}\right] = \frac{P}{V} * \frac{\frac{\ln(10)}{k}}{\log\left({}^{C_0}/_{C}\right)} = \frac{P * t_{0.1}}{V * \log(10)}$$

In this equation, E_{EO} is the electric energy per order and P is the power as the product of average current and average potential. The lower the value of E_{EO}, the more energy efficient the process. These values are shown in Table 6, along with bench and pilot SynGW results for comparison. Table 6 also compares the commercial and pilot reactor results side by side, along with some key reactor parameters.

Table 6 Comparison of 1,4-dioxane degradation rate constants and half-life based on Equations 1 and 3, with ASA_{AO} based on Equation 4 and E_{EO} based on Equation 5 (Radjenovic & Sedlak, 2015).

	rate constant, k [h^{-1}]	half-life, $t_{1/2}$ [h]	current density [mA/cm^2]	ASA_{AO} [$h*m^2/m^3$]	E_{EO} [kWh/m^3]
Bench (constant)	0.067	10.3	11.0	583	508
Pilot (SynGW)	0.150	4.6	10.6	242	315
Pilot (CGW)	0.123	5.6	12.4	305	152
Commercial (CGW)	0.944	0.7	112	28	176

With $ASA_{AO\_commercial}$ = 28 $h*m^2/m^3$, the commercial reactor performs DX removal far more quickly with respect to (apparent) anode surface area than the configurable pilot reactor where ASA_{AO_pilot} = 305 $h*m^2/m^3$. However, considering normalized electrical energy per electrode order, the commercial reactor's result of $E_{EO\_commercial}$ = 176 kW h/m^3 indicates that it is less electrically efficient than the pilot reactor (E_{EO_pilot} = 152 kW h/m^3).

In addition to the different anode geometries and cathode pairs, another major difference between the two reactors is the nature of the anodic material itself: in the pilot reactor a mixed-metal oxide finish has been applied to a titanium substrate whereas in the commercial reactor the Magnéli-phase titanium itself is a very highly conductive surface because of its nature as a sub-stoichiometric oxide of titanium (Smith, Walsh, et al., 1998). Smith et al report that anodes of uncoated Ebonex®, a patented Magnéli-phase Ti material, have a very high oxygen evolution potential (OEP). Table 7 shows the relative OEPs of some electrode materials in acidic solution. Ti-MMO, shown as Ti/IrO_2-Ta_2O_5, has an average OEP about 30% lower than Magnéli-phase titanium dioxide and boron-doped diamond anodes. Lead oxide and platinum anode OEP values are presented for reference.

Table 7 Oxygen evolution potentials in acidic solution for a variety of electrode materials. Table is adapted from Comninellis et al. Note 1 is from Liang (2018). (Comninellis, Kapalka, et al., 2008; Liang, Lin, et al., 2018; Martínez-Huitle & Andrade, 2011; Moreira et al., 2017)

Anode material	O_2 evolution potential [V]
Magnéli phase Ti_4O_7	2.3 - 2.5[1]
BDD	2.2–2.6
Ti/PbO_2	1.8–2.0
Pt	1.6-1.9
Ti/IrO_2-Ta_2O_5	1.5-1.8

It has been reported that the high OEP electrodes generate higher concentrations of reaction byproducts than Ti-MMO electrodes, mainly because of the very high rate of radical production yielding an over-abundance of $^{\bullet}OH$ or chlorine radicals which will react non-selectively with other ions in the reactor solution (Anglada et al., 2009; Bagastyo, Batstone, et al., 2012; Bagastyo et al., 2011). Magnéli-phase titanium oxide, like BDD, is considered to be a non-active anode because of its high overpotential for oxygen evolution, which results in weak interactions between $^{\bullet}OH$ and the anode surface, freeing up the radicals for non-specific reaction with compounds in the bulk solution (Comninellis, 1994; Martínez-Huitle & Andrade, 2011; Panizza & Cerisola, 2009). Some of these reactions result in degraded contaminant, but others result in elevated concentrations of undesirable byproducts. In this study ClO_4^- increased dramatically in the commercial reactor to a final concentration of 0.15 mM in less than 5 hours of electrolytic treatment, compared to a final concentration of 0.84 μM after 18 hours in the Ti-MMO pilot reactor. For the salt-rich CGW of this study, an excess of chloride likely underwent reaction with electro-generated radicals, forming chlorinated organic by-products at a higher concentration in a shorter period in the commercial reactor, due to the higher reactivity of the anode material.

As reported in section 4.2.4., other compounds in addition to 1,4-dioxane were present in the contaminated site water. In Figure 19, above, benzene was removed from the groundwater, and carbon tetrachloride and chloroform both formed as a result of the electrochemical treatment and the liberation of the reactive free radical of chlorine, $^{\bullet}Cl$, from salts present in the contaminated groundwater (Anglada, Urtiaga, et al., 2011). The lag in perchlorate increase is explained by the nature of solution equilibrium: chloride, present initially, was to some extent oxidized during the course of reactor operation to chlorate. As the chlorate concentration increased, further oxidation reactions occurred to transform it to perchlorate. These reactions, taken together, explain the total decrease in chloride ion concentration over the course of reaction time, along with the gradual increase of chlorate and perchlorate (Bergmann et al., 2009; Costa et al., 2009; Schaefer et al., 2015; Zöllig et al., 2015).

The final concentrations of these undesired by-products are presented in Table 9 along with starting values for reference. Several compounds in the final analysis are of concern because they are at levels that are unsafe for human health. In the Third Unregulated Contaminant Monitoring Rule, the US EPA's minimum reporting level for chlorate monitoring was 20 μg/L, though there is not a federally mandated maximum acceptable limit for chlorate in groundwater, mainly because it is understood to be biodegradable in anaerobic conditions so will not persist for long periods in the environment (Cotruvo, 2013; USEPA, 2017d). The US EPA has not yet set an MCL for perchlorate, but several states have adopted limits from 0.8 to 71 μg/L for perchlorate in drinking or groundwater (USEPA, 2017c). As of 2009, carbon tetrachloride has an MCL of 5 μg/L in drinking water (USEPA, 2009). The U.S. Safe Drinking Water Act has defined an MCL of 80 μg/L for the sum of chloroform, bromoform, and bromo- and dibromo-chloromethane combined (USEPA, 2012a). The production of chlorate, perchlorate, and carbon tetrachloride was markedly

greater in the commercial reactor than in the pilot reactor, yet there was greater chloroform production in the pilot than in the commercial reactor. It is likely that because of the abundance of radicals produced by the Magnéli-phase anode, chloroform produced in the commercial reactor was subject to more interaction with chloride radicals, resulting in CCl_4 formation, whereas in the pilot reactor there was not enough of an excess of radicals to push the CCl_4 formation reaction forward.

In the pilot reactor experiment, there was a correlation between increasing temperature and increasing power, as shown in Figure 21. The commercial reactor, with its much smaller anode surface area than the pilot reactor, showed minimal power change despite a greater than 30-degree temperature increase. In the pilot reactor, the increase in power is attributable to an increase in current, since the voltage was steady within about ± 0.5 V in all cases. The current rose by as much as 30 to 40 A over the time span of reaction durations as short as six hours between shutdowns. The pilot reactor with CGW was in a deep chilled water bath, which effectively depressed the starting reaction temperatures and probably helped to limit the current increase. The chilled water bath was implemented following the high power and temperature results with the SynGW experiment, which used a chilled water bath to only about 25% of the reactor's total straight-side height. It was expected that the higher conductivity CGW would have greatly increased reactivity in the electrochemical process, and would generate more heat, so the reactor was placed in a chilled water bath that allowed cooling contact on the entire bottom and 80% of the depth of the reactor. The bath was effective in limiting heat up and suppressing power demands, though it may also have impacted the rate of reaction, at least until the power was increased to deliver the higher current density. These relationships are shown in Figure 11, above. No additional cooling was introduced for the commercial reactor because the small volume and

the recirculation system with its stand-alone vessel were expected to allow for adequate temperature management, however the system was powered down twice due to high temperature.

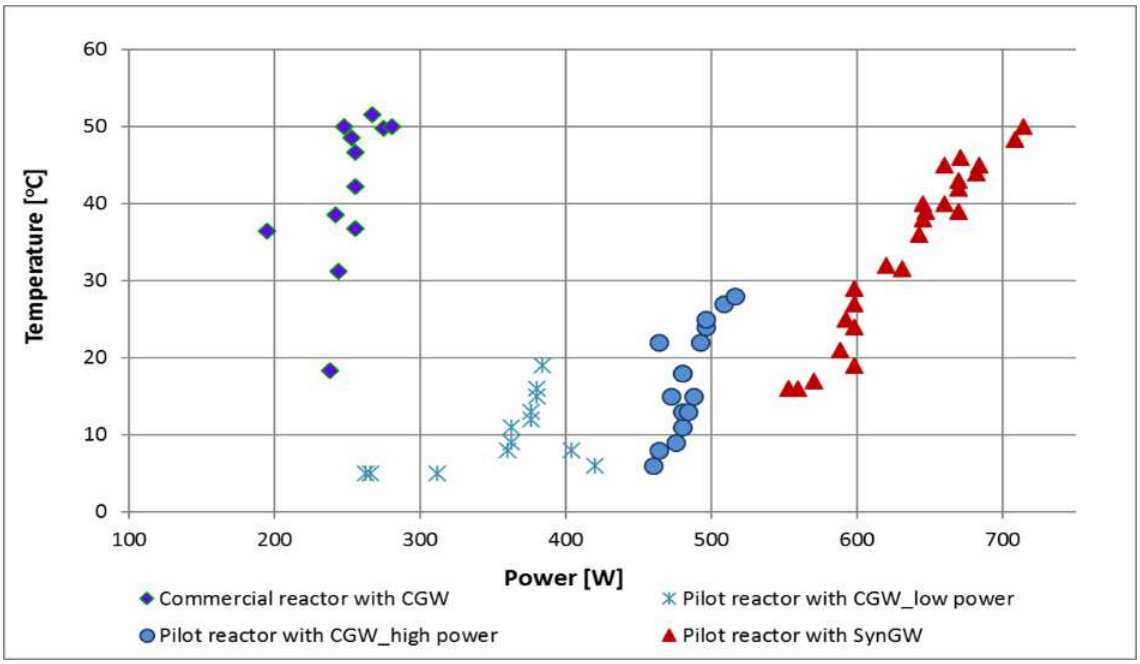

Figure 21 Solution temperature with respect to applied power.

Table 8 Comparison of final concentration with initial concentrations. Units are in µg/L unless explicitly noted otherwise.

Compound	Initial concentration, raw sample, pre-decant	Final concentration, pilot	Final concentration, commercial
chloride LOQ = 0.00111 mg/L	17400-18300 mg/L[1]	16500 mg/L	9620 mg/L
chlorate LOQ =0.0027 mg/L	86-540 mg/L[1]	2680 mg/L	16300 mg/L
perchlorate LOQ = 0.0040 mg/L	nd[2]	nd	0.539 mg/L
chloroform LOQ = 113 µg/L, LOD = 34 µg/L	1310	246000	27500
carbon tetrachloride LOQ = 131 µg/L, LOD = 39 µg/L	nd	nd	4790
benzene LOQ = 30 µg/L, LOD = 9 µg/L	265	nd	nd
1,4-dioxane LOQ = 16 µg/L, LOD = 5 µg/L	626	44	24
chlorobenzene LOQ = 54 µg/L, LOD = 16 µg/L	115	nd	nd
1,4-oxathiane LOQ = 144 µg/L, LOD = 43 µg/L	154	nd	nd
chloropyridine[2] LOQ = 42 µg/L, LOD = 13 µg/L	100	97	14
dichloropyridine[3] LOQ = 86 µg/L, LOD = 26 µg/L	93	nd	29
bis(2-chloroisopropyl) ether LOQ = 206 µg/L, LOD = 62 µg/L	374	nd	nd

[1]range of concentration at the start of processing [2]not detected

[3]as 2-chloropyridine [4]as 3,5-dichloropyridine

6. SUMMARY AND CONCLUSIONS

In bench-scale reactor testing the presence of inter-electrode media did not improve DX removal rates in continuous flow mode. A comparison of treatment kinetics between continuous flow and batch modes showed no significant difference. Furthermore, batch mode results showed that reversing polarity improved the reaction rate by 40%. The DX removal kinetics from the pilot-scale reactor for SynGW were more than 2x faster than the results from the bench-scale reactor at comparable electrode area to volume ratio and current density; however, the mechanisms responsible for this scale-up effect remain to be determined.

In the pilot reactor, the higher-conductivity contaminated site groundwater showed slightly longer 1,4-dioxane half-life than the synthetic groundwater, which may be due to competition for radicals from the much greater ion content in the CGW. Some unwanted reaction by-products such as chloroform and chlorate were detected, but concentrations were generally low enough that post treatment, for instance through microbial reduction, could likely remove them to meet groundwater standards.

The commercial reactor did remove the dioxane more quickly than the static reactor but it also produced more undesirable by-products than the pilot reactor, including carbon tetrachloride and higher concentrations of perchlorate. This greater production of by-products is due mainly to the higher current density applied in that reactor and the nature of the anode material. A comparison of normalized log unit reduction with respect to anode surface area shows the commercial reactor to be more efficient than the pilot reactor at DX removal based on electrode surface area required per log unit removal: $ASA_{AO} = 28\ \mathrm{h{*}m^2/m^3}$ versus $305\ \mathrm{h{*}m^2/m^3}$, respectively. However, the comparison of normalized log unit reduction with respect to power required shows the pilot reactor

to be more efficient, with an E_{EO} value of $152\ \mathrm{kWh/m^3}$, compared to the commercial E_{EO} of $176\ \mathrm{kWh/m^3}$.

In addition to by-product generation, the other main drawback to the use of finely porous Magnéli-phase ceramic as an anode for groundwater treatment is the tendency for plugging. In this investigation, the CGW was carefully decanted to avoid including any visible sediment in the treated volume. For the commercial reactor with its small total volume this was relatively simple to do, with a small total amount of solids held back, but in a larger reactor or at a larger scale, it would be critical to include a settling, flocculation, or filtration step upstream of the reactor. For the pilot reactor, about 16 times the volume was decanted, with at least 500 cm^3 of solids slurry held back. As the treatment volume increases, this untreatable volume will likewise increase. The expanded mesh electrodes would be better able to handle the presence of soil solids without blinding off. The pilot reactor was only tested with decanted solution, however. Further testing of contaminated site groundwater without decanting would yield helpful information for additional scale-up.

Another advantage of the pilot reactor is that it allows for testing with various electrode materials and for using different electrode spacing. Although this study did not exploit the electrode spacing options, future researchers may be able to test different configurations with these reactors.

Ultimately the appropriate solution for groundwater contamination will be dictated primarily by process economics rather than solely by treatment efficiency, so a reactor design that uses standard materials and measurements, is configurable, is straightforward to scale up, and is uncomplicated to maintain will be useful as it will have low capital and installation costs and be relatively low-cost to operate.

7. FUTURE WORK

The investigations conducted in this study illustrated that electrochemical oxidation is a powerful technology for the treatment of water contaminated with the persistent organic pollutant 1,4-dioxane. However, several significant challenges remain. Of key importance for future work is advancing the quantification of control parameters with respect to properties of the contaminated groundwater, with testing using actual site water, and with the goal of implementation in real-world conditions. Development of a predictive relationship between, for example, conductivity and optimal current density, or between suspended solids content and optimal electrode gap will be useful for people working to implement solutions to contaminated groundwater.

The non-flowing reactor may allow treatment to a target set point with minimal additional mechanical equipment, which can be a capital and operating cost benefit. The extent of mixing due to bubble generation was not quantified directly in these experiments, although the general results indicate some good level of mixing. Optimizing and doing more scale-up of this bench-scale reactor will require study of the bulk mixing that is achieved passively from the gas generation at the electrodes, because this will help with better understanding of heat transfer (cooling) requirements and recirculation rates. A passive or recirculating cooling jacket may be operationally more effective than employing traditional recirculation for cooling. An added benefit to using a cooling jacked instead of recirculating the contaminated groundwater is the minimization of potential leaks of the contaminated water from the treatment system. The early work of Wu and Rangaiah on the impacts of bubbles on mass transfer in an electrochemical reactor may be furthered by examining electrode surface geometries with respect to contaminant degradation and by-product production (W. S. Wu & Rangaiah, 1993). The results of additional

work on passive mixing can be applied to a field-scale design in the form of a mobile reactor skid system.

Continued research into electrode coatings and their operational effects with given groundwater parameters or conditions is needed. Progress is constantly being made on development of more efficient materials, but work can be continued to find the optimal electrode for a given groundwater condition, that is, one that efficiently degrades the problem contaminants without producing unacceptable amounts of undesirable reaction by-products. As an example of a novel anode material, doped tin-oxide (commercial name IRSA, Evoqua Water Technologies, Union, NJ) expanded mesh anodes and Magnéli-phase titanium-coated expanded mesh anodes were tested with SynGW, with Ti-MMO cathodes in the complementary positions in each case. As can be seen in Figure 22, the doped tin-oxide anodes increased DX removal rates by a factor of 2.5 compared to Ti-MMO anodes. Detail of this work is attached in the Appendix.

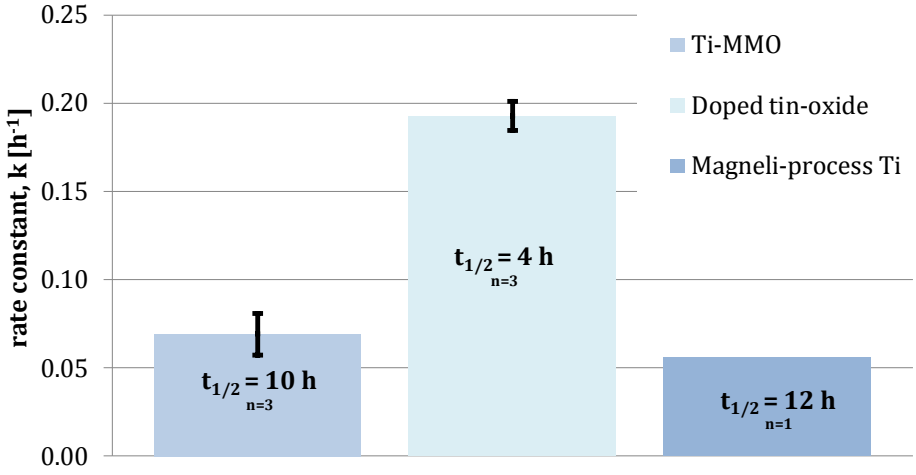

Figure 22 Bench-scale reactor batch mode expanded mesh anode comparison, with Ti-MMO cathodes in each case.

Unknowns to investigate further include the level of filtration required for expanded mesh versus ceramic anodes, and the use of electrochemical oxidation in combination with other treatment systems for more complete removal of the target contaminant, and for removal of undesirable reaction byproducts. For the former, in this study the pilot reactor design's gap between the bottoms of the electrodes and the bottom of the reactor allowed room for solids to settle, once the system was powered down. In a scaled-up design solids would be swept out as the reactor is emptied from a low-point drain valve. But the maximum solids concentration allowable is unknown. Without an understanding of that parameter, additional upstream equipment is required for filtration and/or settling. For the use of electrochemical oxidation in combination with other treatment systems, the impacts of byproducts not only on human health, but also on *in situ* subsurface biota are important to consider in treatment system design, because the downstream microbes may play an important role in further or final degradation of contaminants. Having an outflow that is non-toxic to the microbes is ideal. The less additional treatment required to render the electrochemical oxidation reactor's outflow biologically benign, the fewer additional unit operations will be required, minimizing capital and operating costs.

The benefit of effective operation of an electrolytic reactor which is configurable and does not require many moving parts (e.g. a skid system) is that it can be deployed in a field setting where it can work reliably without requiring a great investment of maintenance attention. The design and operation concept for the field-scale reactor is that it would be filled by a regular submerged pump, as from a well, would be allowed to run to the point of desired contaminant concentration, and then would be pumped out downstream, along the groundwater's regular flow path. Specifically, this would be done by installing a set or series of box-like closed reactors in a dug out rectangular subsurface sump area, to allow the contaminated water to technically remain below grade. The

subsurface treatment units would be accessible so that electrodes may be serviced or changed out as degradation efficiency decreases. There may be a connection to an above-grade modular heat exchanger using water or some other heat transfer fluid for the cooling jacket, depending on the nature of the setting. Water from the contaminated zone would be pumped into the reactor. The pump would be controlled by redundant level sensors to prevent overfilling. Once the reactor was full and electrodes were adequately submerged, sufficient power would be supplied to achieve the desired current density. Vent ports would allow off-gassing of the reaction, with lines that are jacketed or that may pass through a coolant to condense vapors and to allow the condensate to run back down into the reactor, avoiding over-pressuring the system. Sensors could monitor pH, temperature, and conductivity throughout the processing time, and perhaps eventually could detect concentrations of dioxane and degradation byproducts. At this point, though, there is not robust capability for in-line detection of DX, so samples would need to be taken and analyzed at the end of the proscribed reaction time, prior to pumping the solution back into the subsurface, downstream of where it was pulled up. This sampling would ensure that target concentration of DX had been met and that the concentration of undesirables is acceptable before reintroducing the water to the environment. In the case of elevated by-product concentrations, which could be anticipated through laboratory testing of the contaminated site waters prior to skid installation, an additional post treatment unit to treat those particular compounds may be installed just downstream of the EAOP reactor.

Electrochemical oxidation is a viable tool in the treatment of groundwater contaminated with DX, and can be effective across a range of conductivity and co-contaminants. The main advantages are that the systems can be self-contained, can be powered remotely, as by solar cells, and with the right electrodes and optimized current density, should be able to treat to a removal

target. The main drawbacks are that undesirable by-products are formed and must be addressed, and that there is some risk of electrode fouling or scaling depending on the nature of the groundwater being treated. These drawbacks may be overcome with a better understanding of the systems being treated. For 1,4-dioxane and some other recalcitrant organic pollutants, EAOP may be an effective approach to remove at least the majority of the compound, with no need to introduce foreign amendments into the subsurface.

8. REFERENCES

ACGIH. (2015). Threshold Limit Values for Chemical Substances and Physical Agents and Biological Exposure Indices. In. Cincinnati, OH: ACGIH.

Adamson, D. T., Anderson, R. H., Mahendra, S., & Newell, C. J. (2015). Evidence of 1,4-dioxane attenuation at groundwater sites contaminated with chlorinated solvents and 1,4-dioxane. *Environmental Science and Technology, 49*(11), 6510-6518. doi:10.1021/acs.est.5b00964

Adamson, D. T., Mahendra, S., Walker, K. L., Rauch, S. R., et al. (2014). A Multisite Survey To Identify the Scale of the 1,4-Dioxane Problem at Contaminated Groundwater Sites. *Environmental Science & Technology Letters, 1*(5), 254-258. doi:10.1021/ez500092u

Adamson, D. T., Newell, C. J., Mahendra, S., Bryant, D., et al. (2017). *In Situ Treatment and Management Strategies for 1,4-Dioxane-Contaminated Groundwater.* (SERDP Project ER-2307 Final Report). Alexandria, VA.

Adamson, D. T., Piña, E. A., Cartwright, A. E., Rauch, S. R., et al. (2017). 1,4-dioxane drinking water occurrence data from the third unregulated contaminant monitoring rule. *Science of the Total Environment, 596-597*, 236-245. doi:10.1016/j.scitotenv.2017.04.085

Ahsan, A., Kamaludin, M., Rahman, M. M., Anwar, A., et al. (2014). Removal of Various Pollutants from Leachate Using a Low-Cost Technique: Integration of Electrolysis with Activated Carbon Contactor. *Water, Air, & Soil Pollution, 225*(12), 9. doi:10.1007/s11270-014-2163-y

Aieta, E. M., Reagan, K. M., Lang, J. S., McReynolds, L., et al. (1988). Advanced Oxidation Processes for Treating Groundwater Contaminated With TCE and PCE: Pilot-Scale Evaluations. *Journal (American Water Works Association), 80*(5), 64-72.

Aitchison, E. W., Kelley, S. L., Alvarez, P. J. J., & Schnoor, J. L. (2000). Phytoremediation of 1,4-Dioxane by Hybrid Poplar Trees. *Water Environment Research, 72*(3), 313-321. doi:10.2175/106143000X137536

Anderson, R. H., Anderson, J. K., & Bower, P. A. (2012). Co-Occurrence of 1,4-Dioxane with Trichlorothylene in Chlorinated Solvent Groundwater Plumes at U.S. Air Force Installations: Fact or Fiction. *Integrated Environmental Assessment and Management, 8*(4), 731-737. doi:10.1002/ieam.1306

Anglada, Á., Urtiaga, A., & Ortiz, I. (2009). Contributions of Electrochemical Oxidation to Waste Water Treatment: fundamentals and Review of Applications. *Journal of Chemical Technology and Biotechnology, 84*(12), 1747-1755. doi:10.1002/jctb.2214

Anglada, Á., Urtiaga, A., Ortiz, I., Mantzavinos, D., et al. (2011). Boron-doped diamond anodic treatment of landfill leachate: Evaluation of operating variables and formation of oxidation by-products. *Water Research, 45*, 828-838. doi:10.1016/j.watres.2010.09.017

Bachtel, H. J. (1957). U.S.A. Patent No. US2811252 A. U. S. Patent Office.

Bagastyo, A. Y., Batstone, D. J., Kristiana, I., Gernjak, W., et al. (2012). Electrochemical oxidation of reverse osmosis concentrate on boron-doped diamond anodes at circumneutral and acidic pH. *Water Research, 46*, 6104-6112. doi:10.1016/j.watres.2012.08.038

Bagastyo, A. Y., Radjenovic, J., Mu, Y., Rozendal, R. A., et al. (2011). Electrochemical oxidation of reverse osmosis concentrate on mixed metal oxide (MMO) titanium coated electrodes. *Water Research, 45*, 4951-4959. doi:10.1016/j.watres.2011.06.039

Barndõk, H., Hermosilla, D., Cortijo, L., Torres, E., et al. (2014). Electrooxidation of industrial wastewater containing 1,4-dioxane in the presence of different salts. *Environmental Science and Pollution Research International, 21*, 5701-5712. doi:10.1007/s11356-013-2483-2

Beckett, M. A., Hua, I. (2001). Impact of Ultrasonic Frequency on Aqueous Sonoluminescence and Sonochemistry. *Journal of Physical Chemistry A, 105*, 3796-3802. doi:10.1021/jp003226x

Beltrán, F. J. (2003). O3/UV/H2O2 Oxidation Technologies. In M. A. Tarr (Ed.), *Chemical Degradation Methods for Wastes and Pollutants: Environmental and Industrial Applications* (pp. 1-75). New York: Marcel Dekker, Inc.

Bergmann, M. E. H., Rollin, J., & Iourtchouk, T. (2009). The occurrence of perchlorate during drinking water electrolysis using BDD anodes. *Electrochimica Acta, 54*(7), 2102-2107. doi:10.1016/j.electacta.2008.09.040

Bockris, J. O., Reddy, A. K. N. (1998). *Modern Electrochemistry: ionics* (2nd ed. Vol. 1). New York: Springer Science+Business Media.

Brillas, E., Cabot, P.-L., & Casado, J. (2003). Electrochemcial Methods for Degradation of Organic Pollutants in Aqueous Media. In M. A. Tarr (Ed.), *Chemical Degradation Methods for Wastes and Pollutants: Environmental and Industrial Applications* (pp. 235-304). New York: Marcel Dekker, Inc.

Brusseau, M. L., Carroll, K. C., Truex, M. J., & Becker, D. J. (2013). Characterization and Remediation of Chlorinated Volatile Organic Contaminants in the Vadose Zone. *Vadose Zone Journal, 12*(4). doi:10.2136/vzj2012.0137

Butkovskyi, A., Jermaisse, A. W., Leal, L. H., van der Zande, T., et al. (2014). Electrochemical Conversion of Micropollutants in Gray Water. *Environmental Science and Technology, 48*, 1893-1901. doi:10.1021/es404411p

Chaplin, B. P. (2014). Critical Review of Electrochemical Advanced Oxidation Processes for Water Treatment Applications. *Environmental Science: Processes & Impacts, 16*, 1182-1203. doi:10.1039/c3em00679d

Chen, G. (2004). Electrochemical Technologies in Wastewater Treatment. *Separation and Purification Technology, 38*(1), 11-41.

Chiang, S. Y. D., Anderson, R. H., Wilken, M., & Walecka-Hutchison, C. (2016). Practical Perspectives of 1,4-Dioxane Investigation and Remediation. *Remediation Journal, 27*(1), 7-27. doi:10.1002/rem.21494

Chiang, S. Y. D., Glover, E. W. J., Peterman, J., Harrigan, J., et al. (2008). Evaluation of natural attenuation at a 1,4-dioxane-contaminated site. *Remediation, 19*(1), 19-37. doi:10.1002/rem.20189

Chiang, S. Y. D., Mora, R., DiGuiseppi, W. H., Davis, G., et al. (2012). Characterizing the intrinsic bioremediation potential of 1,4-dioxane and trichloroethene using innovative environmental diagnostic tools. *Journal of Environmental Monitoring, 14*(9), 2317-2326. doi:10.1039/c2em30358b

Chitra, S., Paramasivan, K., Cheralathan, M., & Sinha, P. K. (2012). Degradation of 1,4-dioxane using advanced oxidation processes. *Environmental Science and Pollution Research International, 19*, 871-878. doi:10.1007/s11356-011-0619-9

Choi, J. Y., Lee, Y.-J., Shin, J., & Yang, J.-W. (2010). Anodic oxidation of 1,4-dioxane on boron-doped diamond electrodes for wastewater treatment. *Journal of hazardous materials, 179*, 762-768. doi:10.1016/j.jhazmat.2010.03.067

Chopra, A. K., Sharma, A. K., & Kumar, V. (2011). Overview of Electrolytic Treatment: An alternative technology for purification of wastewater. *Archives of Applied Science Research, 3*(5), 191-206.

Comninellis, C. (1994). Electrocatalysis in the electrochemical conversion/combustion of organic pollutants for waste water treatment. *Electrochimica Acta, 39*(11), 1857-1862. doi:10.1016/0013-4686(94)85175-1

Comninellis, C., Kapalka, A., Malato, S., Parsons, S. A., et al. (2008). Advanced oxidation processes for water treatment: advances and trends for R&D. *Journal of Chemical Technology and Biotechnology, 83*, 769-776. doi:10.1002/jctb.1873

Costa, C. R., Montilla, F., Morallón, E., & Olivi, P. (2009). Electrochemical oxidation of acid black 210 dye on the boron-doped diamond electrode in the presence of phosphate ions: Effect of current density, pH, and chloride ions. *Electrochimica Acta, 54*(27), 7048-7055. doi:10.1016/j.electacta.2009.07.027

Cotruvo, J. (2013). Contaminant of the month: chlorate. *Water Technology: Solutions for Industrial Water Management*(April 1, 2013).

CWQCC. (2016). *5 CCR 1002-41: Regulation No. 41 Basic Standards for Ground Water*. Denver, CO: Secretary of State, State of CO.

Davis, E. L. (1997). *How heat can acceleraate in-situ soil and aquifer remediation: Important chemical properties and guidance on choosing the appropriate technique*. (540-S-97-502). Washington, DC: US EPA.

Deng, Y., Englehardt, J. D. (2006). Electrochemical oxidation for landfill leachate treatment. *Waste Management, 27*, 380-388. doi:10.1016/j.wasman.2006.02.004

DiGuiseppi, W., Hatton, J., & Walecka-Hutchison, C. (2017). CleanUp2017 Keynote: 1,4-Dioxane Treatment Technologies.

DiGuiseppi, W., Walecka-Hutchison, C., & Hatton, J. (2016). 1,4-Dioxane Treatment Technologies. *Remediation: the Journal of Environmental Cleanup Costs Technologies & Techniques, 27*(1), 71-92. doi:10.1002/rem.21498

Favara, P., Tunks, J., Hatton, J., & DiGuiseppi, W. (2016). Sustainable Remediation Considerations for Treatment of 1,4-Dioxane in Groundwater. *Remediation Journal, 27*(1), 133-158. doi:10.1002/rem.21501

Ferro, A. M., Kennedy, J., & LaRue, J. C. (2013). Phytoremediation of 1,4-dioxane-containing recovered groundwater. *International Journal of Phytoremediation, 15*, 911-923. doi:10.1080/15226514.2012.687018

Fleming, E. C. (2000). *Advanced Oxidation Processes for Remediation of Explosives-Contaminated Soils.* (Doctor of Philosophy Dissertation), Louisiana State University, Louisiana. (UMI #9979260)

GAMAP. (2009). Groundwater Information Sheet: 1,4-dioxane. In. Sacramento, CA: State of California.

Garcia-Segura, S., Ocon, J. D., & Chong, M. N. (2018). Electrochemical oxidation remediation of real wastewater effluents — A review. *Process Safety and Environmental Protection, 113*(Supplement C), 48-67. doi:10.1016/j.psep.2017.09.014

Gent, D. B., Wani, A., & Alshawabkeh, A. N. (2012). Experimental design for one-dimensional electrolytic reactive barrier for remediation of munition constituent in groundwater. *Electrochimica Acta, 86*, 130-137. doi:10.1016/j.electacta.2012.04.043

Ghatak, H. R. (2014). Advanced oxidation processes for the treatment of biorecalcitrant organics in wastewater. *Critical Reviews in Environmental Science and Technology, 44*, 1167-1219. doi:10.1080/10643389.2013.763581

Gilbert, D. M., Sale, T. C. (2005). Sequential Electrolytic Oxidation and Reduction of Aqueous Phase Energetic Compounds. *Environmental Science & Technology, 29*(23), 9270-9277. doi:10.1021/es051452k

Gilbert, D. M., Sale, T. C., & Petersen, M. A. (2010). Electrolytic Reactive Barriers for Chlorinated Solvent Remediation. In H. F. Stroo & C. H. Ward (Eds.), *In Situ Remediation of Chlorinated Solvent Plumes* (pp. 573-590). New York, NY: Springer New York.

Gomes, H. I., Dias-Ferreira, C., & Ribeiro, A. B. (2013). Overview of in situ and ex situ remediation technologies for PCB-contaminated soils and sediments and obstacles for full-scale application. *Science of the Total Environment, 445-446*(Supplement C), 237-260. doi:10.1016/j.scitotenv.2012.11.098

Gotsi, M., Kalogerakis, N., Psillakis, E., Samaras, P., et al. (2005). Electrochemical oxidation of olive oil mill wastewaters. *Water Research, 39*(2005), 4177-4187. doi:10.1016/j.watres.2005.07.037

Heron, G., Parker, K., Fournier, S., Wood, P., et al. (2015). World's Largest In Situ Thermal Desorption Project: Challenges and Solutions. *Groundwater Monitoring & Remediation, 35*(3), 89-100. doi:10.111/gwmr.12115

Hung, H.-M., Hoffmann, M. R. (1999). Kinetics and Mechanism of the Sonolytic Degradation of Chlorinated Hydrocarbons: Frequency Effects. *Journal of Physical Chemistry A, 103*, 2734-3739. doi:10.1021/jp9845930

Jasmann, J. R. (2016). *Catalytic strategies for enhancing electrochemical oxidation of 1,4-dioxane: TiO2 dark activation and microbial stimulation*. [Doctoral dissertation]. CSU Chemistry, 2014-2016, Fort Collins, CO.

Jasmann, J. R., Borch, T., Sale, T. C., & Blotevogel, J. (2016). Advanced Electrochemical Oxidation of 1,4-dioxane via Dark Catalysis by Novel Titanium Dioxide (TiO2) Pellets. *Environmental Engineering Science and Technology, 50*, 8817-8826. doi:10.1021/acs.est.6b02183

Jasmann, J. R., Gedalanga, P. B., Borch, T., Mahendra, S., et al. (2017). Synergistic treatment of mixed 1,4-dioxane and chlorinated solvent contaminations by coupling electrochemical oxidation with aerobic biodegradation. *Environmental Science and Technology, 51*(21), 12619-12629. doi:10.1021/acs.est.7b03134

Kang, J. W. (2014). Removing environmental organic pollutants with bioremediation and phytoremediation. *Biotechnology Letters, 36*(6), 1129-1139. doi:10.1007/s10529-014-1466-9

Kapałka, A., Fóti, G., & Comninellis, C. (2010). Basic Principles of the Electrochemical Mineralization of Organic Pollutants for Wastewater Treatment. In C. Comninellis & G. Chen (Eds.), *Electrochemistry for the Environment* (pp. 1-23). New York, NY: Springer.

Kim, K., Kuppuswamy, M., & Savinell, R. (2000). Electrochemical oxidation of benzene at a glassy carbon electrode. *Journal of Applied Electrochemistry, 30*(543), 543-549. doi:10.1023/A:100382213

Klančar, A. J. T., Kristl, Albin; Meglič, Andrej; Rozina, Tinkara; Justin, Maja Zupančič; Roškar, Robert. (2016). An advanced oxidation process for wastewater treatment to reduce the ecological burden from pharmacotherapy and the agricultural use of pesticides. *Environmental Engineering, 97*, 186-195. doi:10.1016/j.ecoleng.2016.09.010

Laine, D. F., Cheng, I. F. (2007). The destruction of organic pollutants under mild reaction conditions: A review. *Microchemical Journal, 85*, 183-193. doi:10.1016/j.microc.2006.07.002

Legrini, O., Oliveros, E., & Braun, A. M. (1993). Photochemical processes for water treatment. *Chemical Reviews, 93*(2), 671-698. doi:10.1021/cr00018a003

Lewis, A. (2014). *1,4-Dioxane White Paper*. State of the Science Reports. white paper. Water Research Foundation. Denver, CO.

Li, B., Zhu, J. (2016). Simultaneous degradation of 1,1,1-trichloroethane and solvent stabilizer 1,4-dioxane by a sono-activated persulfate process. *Chemical Engineering Journal, 284*, 750-763. doi:10.1016/j.cej.2015.08.153

Li, S., Bejan, D., McDowell, M. S., & Bunce, N. J. (2008). Mixed first and zero order kinetics in the electrooxidation of sulfamethoxazole at a boron-doped diamond (BDD) anode. *Journal of Applied Electrochemistry, 38*(2), 151-159. doi:10.1007/s10800-007-9413-2

Li, T., Wang, Y., Guo, S., Li, X., et al. (2016). Effect of polarity-reversal on electrokinetic enhanced bioremediaton of pyrene-contaminated soil. *Electrochimica Acta, 187*, 567-575. doi:10.1016/j.electacta.2015.11.097

Liang, S., Lin, H., Yan, X., & Huang, Q. (2018). Electro-oxidation of tetracycline by a Magnéli phase Ti_4O_7 porous anode: Kinetics, products, and toxicity. *Chemical Engineering Journal, 332*(15 January 2018), 628-636. doi:10.1016/j.cej.2017.09.109

Liao, C., Kang, S., & Wu, F. (2001). Hydroxyl radical scavenging role of chloride and bicarbonate ions in the H_2O_2/UV process. *Chemosphere, 44*(5), 1193-1200. doi:10.1016/S0045-6535(00)00278-2

Ma, J. W., Wang, F. Y., Huang, Z. H., & Wang, H. (2010). Simultaneous removal of 2,4-dichlorophenol and Cd from soils by electrokinetic remediation combined with activated bamboo charcoal. *Journal of hazardous materials, 176*, 715-720. doi:10.1016/j.jhazmat.2009.11.093

Mahendra, S., Grostern, A., & Alvarez-Cohen, L. (2013). The impact of chlorinated solvent co-contaminants on the biodegradation kinetics of 1,4-dioxane. *Chemosphere, 91*, 88-92. doi:10.1016/j.chemosphere.2012.10.104

Martínez-Huitle, C. A., Andrade, L. S. (2011). Electrocatalysis in wastewater treatment: recent mechanism advances. *Quimica Para Um Mundo Melhor, 34*(5), 850-858. doi:10.1590/S0100-40422011000500021

Martínez-Huitle, C. A., Ferro, S. (2006). Electrochemical Oxidation of Organic Pollutants for the Wastewater Treatment: direct and indirect processes. *Chemical Society Review, 35*(12), 1324-1340.

Martínez-Huitle, C. A., Rodrigo, M. A. (2015). Single and Coupled Electrochemical Processes and Reactors for the Abatement of Organic Water Pollutants: A Critical Review. *Chemical Reviews, 115*, 13362-13407.

Mena, E., Villaseñor, J., Rodrigo, M. A., & Cañizares, P. (2016). Electrokinetic remediation of soil polluted with insoluble organics using biological permeable reactive barriers: Effect of periodic polarity reversal and voltage gradient. *Chemical Engineering Journal, 299*, 30-36. doi:10.1016/j.cej.2016.04.049

Mohr, T., Stickney, J., & DiGuiseppe, B. (2010). *Environmental Investigation and Remediation: 1,4-dioxane and other solvent stabilizers*. Boca Raton [FL]: CRC Press.

Moreira, F. C., Boaventura, R. A. R., Brillas, E., & Vilar, V. J. P. (2017). Electrochemical advanced oxidation processes: A review on their application to synthetic and real

wastewaters. *Applied Catalysis B: Environmental, 202*(March 2017), 217-261. doi:10.1016/j.apcatb.2016.08.037

Nakajima, A., Tanaka, M., Kameshima, Y., & Okada, K. (2004). Sonophotocatalytic destruction of 1,4-dioxane in aqueous systems by HF-treated TiO_2 powder. *Journal of Photochemistry and Photobiology A: Chemistry, 167*, 75-79. doi:10.1016/j.jphotochem.2004.04.013

Nakamiya, K., Hashimoto, S., Ito, H., Edmonds, J. S., et al. (2005). Degradation of 1,4-dioxane and cyclic ethers by an isolated fungus. *Applied and Environmental Microbiology, 71*(3), 1254-1258. doi:10.1128/AEM.71.3.1254-1258.2005

NHDES. (2011). Environmental Fact Sheet: 1,4-dioxane and Drinking Water. In B. o. H. R. A. New Hampshire Department of Environmental Services (Ed.), (Vol. ARD-EHP-30, pp. 3). Concord, NH.

Oberle, D., Crownover, E., & Kluger, M. (2015). *In Situ* Remediation of 1,4-dioxane Using Electrical Resistance Heating. *Remediation, 25*(2), 35-42. doi:10.1002/rem.21422

Oliveira, R. T. S., Salazar-Banda, G. R., Santos, M. C., Calegaro, M. L., et al. (2007). Electrochemical oxidation of benzene on boron-doped diamond electrodes. *Chemosphere, 66*(11), 2152-2158. doi:10.1016/j.chemosphere.2006.09.024

Panizza, M., Cerisola, G. (2009). Direct and Mediated Anodic Oxidation of Organic Pollutants. *Chemical Reviews, 109*(12), 6541-6569.

Petering, W. H., Aitchison, A. G. (1945). U.S.A. Patent No. US2371644 A. U. S. Patent Office.

Petersen, M. A., Reardon, K. F. (2009). Effect of Gas Evolution on Mixing and Conversion in a Flow-Through Electrochemical Reactor. *AIChE Journal, 55*(9), 2468-2476. doi:10.1002/aic.11827

Petersen, M. A., Sale, T. C., & Reardon, K. F. (2007). Electrolytic trichloroethene degradation using mixed metal oxide coated titanium mesh electrodes. *Chemosphere, 67*(2007), 1573-1581. doi:10.1016/j.chemosphere.2006.11.056

Radjenovic, J., Sedlak, D. L. (2015). Challenges and Opportinities for Electrochemcial Processes as next-generation Technologies for the Treatment of Contaminated Water. *Environmental Science and Technology, 49*, 11292-11302.

Rajeshwar, K., Ibanez, J. G., & Swain, G. M. (1994). Electrochemistry and the environment. *Journal of Applied Electrochemistry, 24*(1077). doi:10.1007/BF00241305

Rao, N. N., Somasekhar, K. M., Kaul, S. N., & Szpyrkowicz, L. (2001). Electrochemical oxidation of tannery wastewater. *Journal of Chemical Technology and Biotechnology, 76*(11), 1124-1131. doi:10.1002/jctb.493

Rapp, D. E. (1960). USA Patent No. US2923747 A. U. S. Patent Office.

Röhrs, J., Ludwig, G., & Rahner, D. (2002). Electrochemically induced reactions in soils: a new approach to the in-situ remediation of contaminated soils? Part 2: remediation experiments with a natural soil containing highly chlorinated hydrocarbons. *Electrochimica Acta, 47*(9), 1405-1414. doi:10.1016/S0013-4686(01)00855-6

Sale, T. C., Gilbert, D. M. (2002). USA Patent No. US 6342150 B1. U. S. Patent Office.

Santos, I. D., Dezotti, M., & Dutra, A. J. B. (2013). Electrochemical treatment of effluents from petroleum industry using a Ti/RuO2 anode. *Chemical Engineering Journal, 226*(Supplement C), 293-299. doi:10.1016/j.cej.2013.04.080

Sathishkumar, P., Mangalaraja, R. V., & Anandan, S. (2016). Review on the recent improvements in sonochemical and combined sonochemcial oxidation processes: A powerful tool for destruction of environmental contaminants. *Renewable and Sustainable Energy Reviews, 55*, 426-454. doi:10.1016/j.rser.2015.10.139

Schaefer, C. E., Andaya, C., Burant, A., Condee, C. W., et al. (2017). Electrochemical treatment of perfluorooctanoic acid and perfluorooctane sulfonate: Insights into mechanisms and application to groundwater treatment. *Chemical Engineering Journal, 317*(Supplement C), 424-432. doi:10.1016/j.cej.2017.02.107

Schaefer, C. E., Andaya, C., & Urtiaga, A. (2015). Assessment of disinfection and by-product formation during electrochemical treatment of surface water using a Ti/IrO_2 anode. *Chemical Engineering Journal, 264*, 411-416. doi:10.1016/j.cej.2014.11.082

Schmalz, V., Dittmar, T., Haaken, D., & Worch, E. (2009). Electrochemical disinfection of biologically treated wastewater from small treatment systems by using boron-doped diamond (BDD) electrodes – Contribution for direct reuse of domestic wastewater. *Water Research, 43*(20), 5260-5266. doi:10.1016/j.watres.2009.08.036

Schuchmann, H.-P., Von Sonntag, C. (1990). The 185 nm photolysis of 1,4-dioxan in aqueous solution in the presence of N_2O: N_2 formation via dioxan photoionization or photoexcitation? *Journal of Photochemistry and Photobiology A: Chemistry, 52*(1), 97-109. doi:10.1016/1010-6030(90)87095-S

Sekar, R., DiChristina, T. J. (2014). Microbially driven Fenton reaction for degradation of the widespread environmental contaminant 1,4-dioxane. *Environmental Science and Technology, 48*, 12858-12867. doi:10.1021/es503454a

Sekar, R., Taillefert, M., & DiChristina, T. J. (2016). Simultaneous transformation of commingled trichloroethylene, tetrachloroethylene, and 1,4-dioxane by a microbially driven Fenton reaction in batch liquid cultures. *Applied and Environmental Microbiology, 82*(21), 6335-6343. doi:10.1128/AEM.02325-16

Shen, W., Chen, H., & Pan, S. (2008). Anaerobic biodegradation of 1,4-dioxane by sludge enriched with iron-reducing microorganisms. *Bioresource Technology, 99*(7), 2483-2487. doi:10.1016/j.biortech.2007.04.054

Smith, J. R., Walsh, F. C., & Clarke, R. L. (1998). Electrodes based on Magnéli phase titanium oxides: the properties and applications of Ebonex® materials. *Journal of Applied Electrochemistry, 28*(10), 1021-1033. doi:10.1023/a:1003469427858

Stefan, M. I., Bolton, J. R. (1998). Mechanism of the Degradation of 1,4-Dioxane in Dilute Aqueous Solution Using the UV/Hydrogen Peroxide Process. *Environmental Science & Technology, 32*(11), 1588-1595. doi:10.1021/es970633m

Suthersan, S., Quinnan, J., Horst, J., Ross, I., et al. (2016). Making Strides in the Management of "Emerging Contaminants". *Groundwater Monitoring & Remediation, 36*(1), 15-25. doi:10.1111/gwmr.12143

Teaf, C. M., Garber, M. M. (2015). *Toxicology and environmental regulation of 1,4-dioxane*. Paper presented at the Contaminated Soils, Sediments, Water and Energy. Conference paper retrieved from

USEPA. (2006). *Treatment Technologies for 1,4-Dioxane: Fundamentals and Field Applications*. (EPA-542-R-06-009). Cinncinati, OH: US EPA National Service Center for Environmental Publications.

USEPA. (2009). *National Primary Drinking Water Regulations* (EPA 816-F-09-004). National Service Center for Environmental Publications.

USEPA. (2012a). *2012 Edition of the Drinking Water Standards and Health Advisories*. (EPA 822-S-12-001). Washington DC: US EPA.

USEPA. (2012b, 3/6/2012). Water: Monitoring & Assessment.

USEPA. (2014). *Technical Fact Sheet: 1,4-dioxane*. (EPA 505-F-14-011). EPA.gov.

40 CFR 136 Subchapter D: Water Programs, (2015).
USEPA. (2017a). *Regional Screening Level (RSL) Chemical-specific Parameters Supporting Table*. Washington, DC: EPA.gov.
USEPA. (2017b). *Regional Screening Level (RSL) Resident Soil to GW Table*. Washington, DC: EPA.gov.
USEPA. (2017c). *Technical Fact Sheet: Perchlorate*. (EPA 505-F-17-003). EPA.gov.
USEPA. (2017d). *The Third Unregulated Contaminant Monitoring Rule (UCMR 3) Data Summary, January 2017*. Washington, DC: USEPA.
Vanýsek, P. (2017). "Equivalent Conductivity of Electrolytes in Aqueous Solution" in CRC Handbook of Chemistry and Physics. In (98th Edition (Internet Version 2018) ed.). Boca Raton, FL: CRC Press/Taylor & Francis.
Villanueva, C. M., Kogevinas, M., Cordier, S., Templeton, M. R., et al. (2014). Assessing Exposure and Health Consequences of Chemicals in Drinking Water: Current State of Knowledge and Research Needs. *Environmental Health Perspectives, 122*(3), 213-221. doi:10.1289/ehp.1206229
Weber, R., Watson, A., Forter, M., & Oliaei, F. (2011). Persistent organic pollutants and landfills: a review of past experiences and future challenges. *Waste management & Research, 29*(1), 107-121. doi:10.1177/0734242X10390730
Wenzel, W. W. (2009). Rhizosphere processes and management in plant-assisted bioremediation (phytoremediation) of soils. *Plant and Soil, 321*(1-2), 385-408. doi:10.1007/s11104-008-9686-1
Woodard, S., Mohr, T., & Nickelsen, M. G. (2014). Synthetic Media: A Promising New Treatment Technology for 1,4-Dioxane. *Remediation, 24*(4), 27-40. doi:10.1002/rem.21402
Wu, W., Huang, Z.-H., & Lim, T.-T. (2014). Recent development of mixed metal oxide anodes for electrochemical oxidation of organic pollutants in water. *Applied Catalysis A: General, 480*, 58-78. doi:10.1016/j.apcata.2014.04.035
Wu, W. S. Rangaiah, G. P. (1993). Effect of Gas Evolution on Mass-Transfer in an Electrochemical Reactor. *Journal of Applied Electrochemistry, 23*(11), 1139-1146. doi:10.1007/Bf00625587
Yan, N., Liu, F., Chen, Y., & Brusseau, M. L. (2016). Influence of groundwater constituents on 1,4-dioxane degradation by a binary oxidant system. *Water, Air, & Soil Pollution, 227*(436). doi:10.1007/s11270-016-3146-y
Zenker, M. J., Borden, R. C., & Barlaz, M. A. (2003). Occurrence and treatment of 1,4-dioxane in aqueous environments. *Environmental Engineering Science, 20*(5), 423-432. doi:10.1089/109287503768335913
Zhang, S., Gedalanga, P. B., & Mahendra, S. (2017). Advances in bioremediation of 1,4-dioxane-contaminated waters. *Journal of Environmental Management, 204*(Part 2), 765-774. doi:10.1016/j.jenvman.2017.05.033
Zöllig, H., Remmele, A., Fritzsche, C., Morgenroth, E., et al. (2015). Formation of chlorination byproducts and their emission pathways in chlorine mediated electro-oxidation of urine on active and nonactive type anodes. *Environmental Science & Technology, 49*, 11062-11069. doi:10.1021/acs.est.5b01675

APPENDIX

Bench-scale reactor supplemental information.

In the bench-scale reactor, the desk-top DC power supply had internal controls which allowed it to maintain constant current and voltage, within ± 0.1 amp and ±0.3 volts over the duration of a 10-hour experiment.

Kinetic models were evaluated using linear regression in Microsoft Excel and in R, with results in full agreement. The output from R for batch reactor no-flow, constant polarity experiments is shown in Table A1.

Table A1 Output from R for the evaluation of data fit to first-order model.

```
Call:
lm(formula = k ~ t, data = fo)

Residuals:
       1        2        3        4        5        6        7
-0.020479  0.043918 -0.042385 -0.039391  0.078629  0.006314 -0.026607

Coefficients:
             Estimate      Std. Error       t value       Pr(>|t|)
(Intercept)  2.048e-02      2.695e-02          0.76         0.482
t           -1.153e-03      9.102e-05        -12.67         5.44e-05 ***
---

Signif. codes:  0 ‘***’ 0.001 ‘**’ 0.01 ‘*’ 0.05 ‘.’ 0.1 ‘ ’ 1

Residual std error:    0.05025 on 5 degrees of freedom
Multiple R-squared:    0.9698
Adjusted R-squared:    0.9638
F-statistic:   160.5 on 1 and 5 DF
p-value:       5.444e-05
```

Figure A1 shows that dioxane degradation progresses most rapidly with regularly reversing electrode polarity as compared to maintaining constant polarity for the duration of the experiment. The control cases showed minor reduction in dioxane concentration over the duration of the experimental period, with the gas sparge case having a slightly lower final concentration.

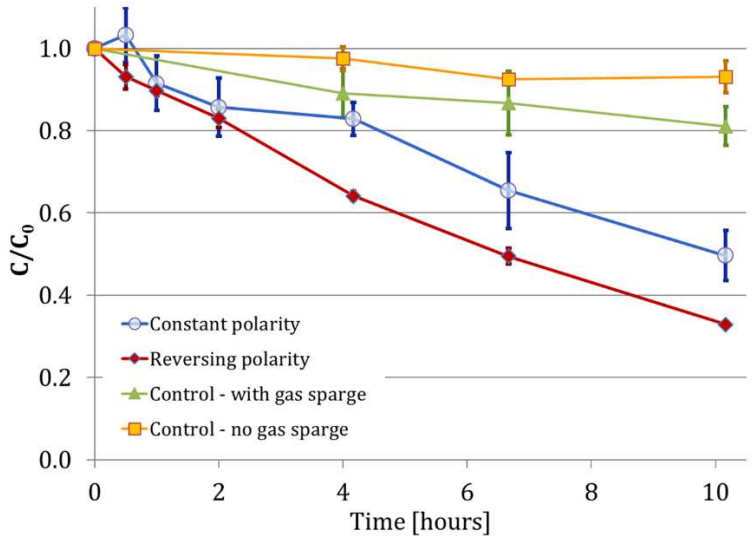

Figure A1 Bench-scale batch reactor results for Ti-MMO electrodes. Error bars shown are standard deviations based on triplicates.

A set of batch experiments was performed using other expanded mesh anodes in combination with expanded mesh Ti-MMO cathodes. The anodes compared in one set of triplicate experiments were doped tin-oxide (trade name IRSA). The other anode material tested was Magnéli-phase titanium, for which a single experiment was performed. The results, summarized in Figure 22, show that the IRSA anode is most effective at dioxane degradation because it has the highest dioxane removal reaction rate constant, thus gives the shortest dioxane half-life of the three materials tested.

Pilot-scale reactor supplemental information

Because this reactor was covered by a lid, sampling during the SynGW experiments was done by slightly lifting up and moving the lid so that it set horizontally flat but somewhat askew from the vertical planes of the sides of the reactor. This created an opening that was large enough to insert a plastic pipette tip into the gap to take a sample. Samples were to be taken from different

points in the reactor's top layer to help quantify the degree of DX concentration uniformity within the reactor. This reactor configuration had no forced mixing so samples were taken from different areas of the reactor as shown in Figure A2 to learn whether sample location had an impact on analytical results, specifically with respect to the key parameter of dioxane concentration. As shown by the natural log of relative concentration over time in Figure A3 the sample location has negligible effect on the measured concentration.

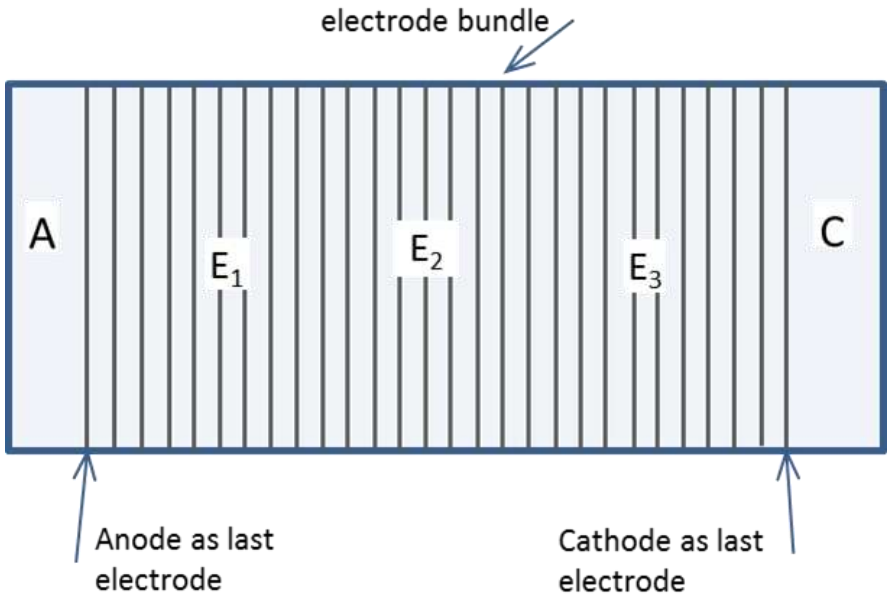

Figure A2 Pilot reactor schematic showing sample points used in the SynGW experiment. The open area to the left of the last anode is the "anode end" and the open area to the right of the last cathode is the "cathode end" as reported in the plot in Figure B. The electrode bundle has sample locations E_x represented by the electrode bed data in Figure B.

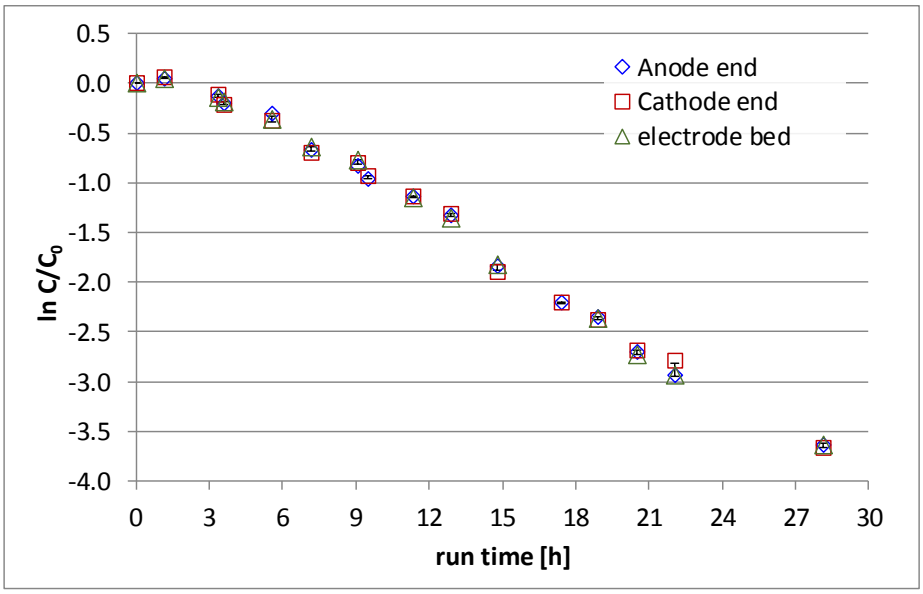

Figure A3 Synthetic groundwater dioxane degradation sampling results with respect to reactor location, showing very close dioxane concentration results for all sample locations. Error bars are for the average of all sample points.

Based on pseudo first-order kinetics, the observed reaction rate constant, k_{obs}, for the linear relationship of dioxane removal from synthetic groundwater is 0.15 h^{-1} as shown in Figure A4. Using Equation 3 this reaction rate constant translates to dioxane half-life of 5 h. Overall 95% of 1,4-dioxane was removed from the SynGW solution over the course of the total 23 hours of electrochemical reaction time with Ti-MMO electrodes at an average current density of 10.7 mA/cm^2. In absolute terms, 58 mg DX was removed. The initial concentration, C_0, was 1 mg/L 1,4-dioxane in 61 L of SynGW solution, and the final concentration was 0.05 mg/L in 60.9 L of solution. The yellow point in the plot shows the $\ln(C/C_0)$ value after regular operation was ended and the system was operated with polarity switching for 5 hours. Disinfection by-products were not analyzed in this case.

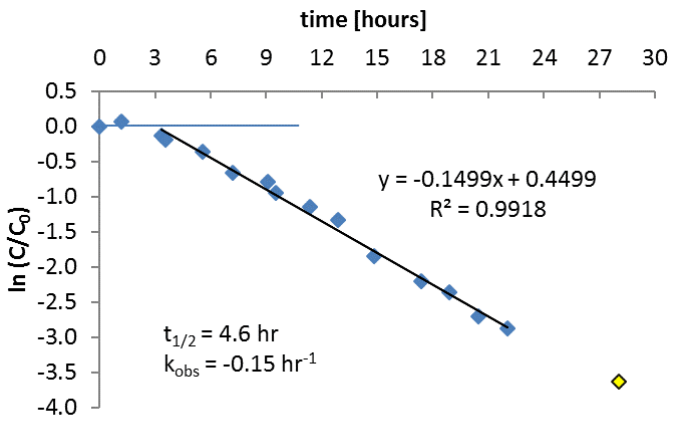

Figure A4 Pilot reactor reaction kinetics plot for SynGW showing a pseudo first-order relationship in the log change of 1,4-dioxane concentration with respect to time. Rate constant k = 0.15 h^{-1}, and $t_{1/2}$ = 4.6 h. The yellow point at about 28 hours is the value after an additional 5 hours operational time with polarity switching.

In Figure A5 the parameters that were tracked over the course of the SynGW experiments are reported, including temperature, pH, 1,4-dioxane concentration, total power, and current density. Because of issues with heat-up, the system was periodically shut down to allow for solution temperature to decrease. The temperature data, as a sinusoidal saw tooth progression of points, is shown in plot a. of Figure A5. The breaks in operation are shown in the figure by the four vertical lines running across the plots. The effects are most marked in the temperature plot (A5.a.) where the temperature falls back down after reaching highs above 40 °C. The time reported on these plots is active (powered-up) time only, not total elapsed time.

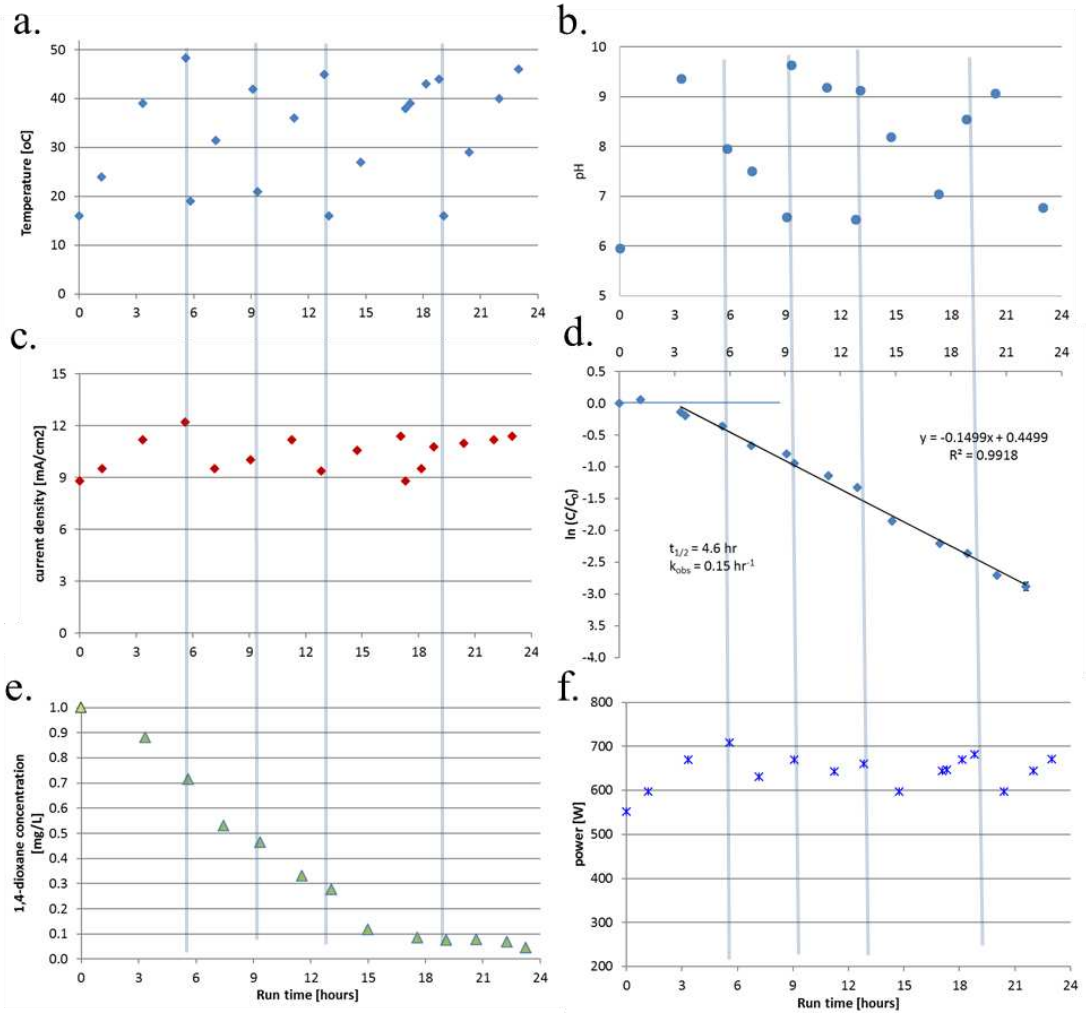

Figure A5 Pilot reactor data parameters for SynGW over the total operational time. Vertical bars on the figure indicate power interruptions. Parameters are shown with respect to time: a.) Temperature, b.) pH, c.) Current density, d.) Log plot of normalized concentration, e.) 1,4-dioxane concentration, and f.) Total power.

Arrhenius equation for the relationship of reaction rate to temperature.

Equation A1

$$k = A * e^{-E_a/RT}$$

where k = rate constant [time^{-1}]
A = frequency factor [time^{-1}]
E_a = activation energy [kJ/mol]
R = universal gas constant [kJ/(mol*K)]
T = temperature [K]